**Anti-Tumor Effects of TRAIL-Expressing Mesenchymal Stromal Cells in a Mouse Xenograft Model of Human Mesothelioma**

Melissa J. Lathrop PhD[1,6], Elizabeth K. Sage MD[4,6], Sherrill L. Macura PhD[2], Elice M. Brooks BS[1], Fernanda Cruz PhD[1], Nick R. Bonenfant BA[1], Dino Sokocevic BA[1], Max B. MacPherson BA[2], Stacie L. Beuschel BS[2], Chad W. Dunaway MD[3], Arti Shukla PhD[2], Samuel M. Janes MD[4], Chad Steele MD[3], Brooke T. Mossman PhD[2], Daniel J. Weiss MD PhD[1,5]


1. Department of Medicine, Pulmonary, University of Vermont, Burlington Vermont
2. Department of Pathology, University of Vermont, Burlington, Vermont
3. Department of Medicine, School of Medicine University of Alabama at Birmingham
4. Lungs for Living Research Centre, UCL Respiratory, University College London, London, UK
5. Corresponding Author
6. Co-First Authors


Corresponding Author:
Daniel J. Weiss, M.D. Ph.D. (dweiss@uvm.edu)
University of Vermont
C317 Given Building
89 Beaumont Ave
Burlington, VT 05405

Melissa Lathrop (mlathrop79@gmail.com)
Sherrill Lathrop Macura (sherrilllathrop@gmail.com)
Elice Brooks (EBrooks@greenmoab.com)
Nicholas Bonenfant (Nicholas.Bonenfant@med.uvm.edu)
Dino Sokocevic (dinosokocevic@gmail.com)
University of Vermont
C352 Given Building
Burlington, VT 05405
Phone: 802-656-8110
Fax:    802-656-8926

Elizabeth K Sage (bethsage@hotmail.co.uk)
Sam M Janes (s.janes@ucl.ac.uk)
University College London
London, UK
Phone: (+44) 020 7679 6975

Chad W. Dunaway (cwardun@uab.edu)
Chad Steele (chadsteele@uab.edu)
Department of Medicine
School of Medicine
University of Alabama at Birmingham
1900 University Blvd, THT 437A
Birmingham, AL 35294

**Effects of TRAIL-Expressing MSCs on Mesothelioma**

Max MacPherson (maximilian.macpherson@med.uvm.edu)
Stacie Beuschel (stacie.beuschel@med.uvm.edu)
Arti Shukla (arti.shukla@med.uvm.edu)
Brooke Mossman (brooke.mossman@med.uvm.edu)
University of Vermont
215 HSRF Building
Burlington, VT  05405
Phone: 802-656-0535
Fax:    802-656-8926

Running Title: Effects of TRAIL-Expressing MSCs on Mesothelioma

## Abstract

Malignant mesothelioma (MM) remains a highly deadly malignancy with poor treatment option. The MM cells further promote a highly inflammatory microenvironment which contributes to tumor initiation, development, severity, and propagation. We reasoned that the anti-inflammatory actions of mesenchymal stromal cells (MSCs) and further anti-tumor effects of MSCs engineered to over-express TNF-related apoptosis inducing ligand (TRAIL) protein (MSC-TRAIL) would effectively inhibit mesothelioma growth. Using a mouse xenograft model of intraperitoneal human mesothelioma, native mouse (mMSC) or human (hMSC) MSCs were administered either systemically (IV) or intraperitoneally (IP) at various times following tumor inoculation. Both mMSCs and hMSCs localized at sites of MM tumor growth *in vivo* and decreased local inflammation. Further, a trend towards decrease in tumor burden was observed. Parallel studies of *in vitro* exposure of nine primary human mesothelioma cell lines to mMSCs or hMSCs demonstrated reduced tumor cell migration. In contrast MSC-TRAIL exposure induced apoptosis of TRAIL sensitive MM cells *in vitro* and both mouse and human MSC-TRAIL significantly reduced the inflammatory tumor environment *in vivo*. Moreover human MSC-TRAIL administration significantly reduced peritoneal tumor burden *in vivo* and increased tumor cell apoptosis. These proof-of-concept studies suggest that TRAIL-expressing MSCs may be useful against malignant mesothelioma.

## Introduction

Malignant mesothelioma (MM) is a devastating malignancy causally associated with exposure to asbestos fibers (1). Development of MM is associated with high levels of local pleural or peritoneal inflammation, particularly driven by the innate immune system (2-4). The long latency of tumor development (30-40 years) and the late stage at which most patients are diagnosed contributes to the brief median survival rate (12 months) (5). The most potent currently available regimen, cisplatinum/pemetrexed, has only extended survival an additional six months, compared to untreated patients or three months compared to patients receiving cisplatinum alone (6). Further, the regimen has significant toxicities and quality of life remains poor for most patients. A variety of other therapeutic approaches, including radiation, surgery, other drug combinations, immunotherapy, and gene transfer-mediated interferon-$\beta$ have not significantly changed overall morbidity and mortality (7). Therefore novel therapies are desperately needed.

Mesenchymal stromal cells (MSCs) are a heterogenous population of multipotent adult cells originally isolated from bone marrow and now found to be present in a wide range of tissues including adipose, placenta, and others (8). Current data suggests that some populations of MSCs exist as pericytes lining blood vessels where they function to modulate local inflammation (9). Isolated MSCs have been intensely studied for use in tissue regeneration and repair particularly in the context of potent immunomodulatory effects on the proliferation and function of a wide range of immune effector cells (10-14). This occurs mostly through paracrine release of soluble mediators but increasing evidence suggests a wider range of MSC activities involving both release of microsome particles and also direct transfer of mitochondria and other intracellular contents through cell-cell bridges (8, 15). Further, as MSCs do not constitutively express critical cell surface antigens involved in immune recognition and rejection, non-human leukocyte antigen matched administration of allogeneic MSCs has been increasingly investigated in a wide range of clinical immune and inflammatory disorders including graft vs host disease, Crohn's disease, and rheumatoid arthritis (16, 17). In parallel, a rapidly growing

number of studies suggest that MSCs, either through innate anti-inflammatory actions, or when engineered to express anti-tumor agents, can have significant effects in reducing tumor burden, metastatic disease, and tumor associated inflammatory microenvironments (18-25). However, there are only limited investigations of MSC actions in pre-clinical models of MM.

Tumor necrosis factor related apoptosis inducing ligand (TRAIL) is a naturally occurring protein which functions to induce apoptosis by binding to the death receptor proteins expressed primarily on malignant cells (26). MM cell lines exhibit variable levels of susceptibility to TRAIL-induced apoptosis and recombinant TRAIL combined with chemotherapy was shown to be more effective in inhibiting tumor growth *in vitro* and in animal models (27, 28). We therefore reasoned that the anti-inflammatory actions of MSCs combined with TRAIL expression might have significant effects on reducing MM tumor burden and associated inflammation. To assess this, we evaluated MSC effects on tumorigenic properties of eleven MM cell lines *in vitro,* and in parallel, the effects of both mouse and human bone marrow-derived MSCs and of MSCs engineered to over-express TRAIL on tumor burden and inflammatory environment in a xenograft model following intraperitoneal injection of human MM cells into severe combined immune deficient (SCID) mice. Despite lack of adaptive immunity, these mice maintain innate inflammatory responses relevant to MM pathogenesis and are thus a good initial model for assessing MSC effects on human mesothelioma cells *in vivo* (2)

## Materials and Methods

### Cell culture

Murine and human bone marrow MSCs (mMSCs, hMSCs) were obtained from the Texas A&M Stem Cell Core facility. These cells have previously been extensively characterized for cell-surface marker expression and differentiation capacity (14, 29). For localization experiments, MSCs stably transduced to express cytoplasmic green fluorescent protein (GFP) were utilized (14, 29). For TRAIL studies mMSCs transfected and selected for constitutive stable expression and hMSCs transduced to express doxycycline-inducible human TRAIL protein (hMSC-FLT) were utilized (14, 29). All MSCs were used at passages 7-8.

The pleural MM cell lines HMESO and H2373 have previously been described (2, 30). Seven additional previously described human peritoneal MM cell lines HAY, YOU, ROB, ORT, PET, PRO, and HEC (28) were generously provided by Dr. Claire Verschraegen (Vermont Cancer Center, University of Vermont). Human pleural MM cell lines CRL-5820 and CRL-5915 are commercially available lines from ATCC (31).

### *In vitro* analysis of tumorigenicity

MSC effect on MM cell tumorigenic properties of proliferation, migration, invasion, cytokine production, and anchorage independent growth were assessed as previously described (2).

### SCID mouse xenograft model of human malignant mesothelioma

All animal procedures were approved by the UVM IACUC and conformed to all appropriate institutional and AAALAC standards. A previously established model of intraperitoneal (IP) inoculation of human HMESO cells into SCID mice was utilized (2). In brief, HMESO cells ($5x10^6$ for localization/tumor development experiments, $1x10^6$ cells for MSC treatment experiments), in sterile

saline were injected IP into male, 6 week old Fox Chase SCID mice (Charles River Laboratories, Boston, MA) (2, 32).

To assess MSC localization to tumors, or effect on the inflammatory microenvironment and tumor development, $1 \times 10^6$ MSCs or PBS (control) were injected either systemically (tail vein [IV]) or IP on day 27, or 7 and 14, respectively, with analysis on day 28. To assess MSC effects on peritoneal inflammation and tumor burden, tumor inoculated mice received IP injections starting day 21, twice a week for 3 weeks. Mice received either control injections of saline (n=6), or $3 \times 10^5$ MSCs in the following groups: MSC-Alone - unmodified mMSCs or hMSCs (n=8 each); MSC-Vector cells - mMSCs transfected with empty vector pCMV6-XL5 (n=8), or hMSC-FLT cells not stimulated with DOX (n=8); MSC-TRAIL cells - mMSC-TRAIL (clone 87) (n=8), or hMSC-FLT cells stimulated for 72 hrs with DOX (n=8). Peritoneal inflammation was assessed by measure of peritoneal lavage fluid (PLF) total cell counts and differentials and content of inflammatory cytokines (mouse and human) (2, 32). Tumor burden was assessed by collection of all tumors, including any small metastatic nodes, with detailed examination of the peritoneal and pleural cavity walls and organs (2, 32). Tumor apoptosis was assessed by TUNEL staining.

**Statistical analysis**

Data was evaluated by analysis of variance (ANOVA) using the Fishers LSD procedure for adjustment of multiple comparisons to the saline treatment groups and considered significant at $p \leq 0.05$ (33). p-values approaching significance noted in the figures refer to comparisons with saline controls only.

Further details on all experimental approaches are provided in the supplemental methods section.

**Results**

**MSCs affect migration but not proliferation, invasiveness, or anchorage independent growth of MM cell lines.**

We initially ascertained that neither mouse nor human MSCs were induced to differentiate by MM medium components and were not killed in direct co-cultures with MM cell lines (data not shown). The growth rate of the pleural MM cell lines HMESO or H2373 over 4-7 days of Transwell exposure was not significantly altered by exposure to soluble mediators from either hMSCs or mMSCs (**Figure 1A**). The proliferation rate of seven additional peritoneal MM cell lines was determined and categorized as either robust, moderate, or weak (**Supplemental Figure 1A**). Proliferation of the robust group HAY and ORT cells was not changed during Transwell exposure to MSC soluble mediators over days 4-7 (**Supplemental Figure 1B**). Both mMSCs and hMSCs significantly inhibited the migration capacity of the four most migratory MM cell lines (HMESO, H2373, CRL5820, and CRL5915), following Transwell exposure for 5 days (**Figure 1B**). Assessment of six other cell lines, HAY, HEC, ORT, ROB, YOU, and PET, demonstrated that HAY and HEC were significantly inhibited only by mMSCs and hMSCs, respectively, while the other lines did not migrate sufficiently to determine an impact by MSCs (**Supplemental Figure 1C**). All 11 cell lines exhibited only weak ability to invade across a basement membrane and no effect of exposure to either mMSC or hMSC by Transwell exposure was observed (**Figure 1C, Supplemental Figure 1D**). Culture of the 11 MM cell lines in anchorage independent growth assays identified that only six of the cell lines were capable of growing colonies of significant size over 14 days (data not shown). MSCs inoculated alone into the culture system did not proliferate or form colonies and thus did not appear to contribute to the number of colonies observed (**Figure 1D**). Co-plating an equal number of MSCs with the HMESO cells determined that there was no change in the size or morphology of colonies formed, and the number of live cells was unaltered (**Figure 1D**). These combined data indicated that exposure to MSCs does not apparently increase the tumorigenicity of MM

cells.  Conversely, release of the soluble cytokines TNF-α, RANTES, and Interleukin-10 by MSCs was not affected by *in vitro* exposure to the 11 MM lines tested (**Supplemental Figure 1E**).

**MSCs home to MM tumors and alter the tumor microenvironment in SCID mice.**

To assess whether MSCs would localize to MM tumors *in vivo*, HMESO tumor-bearing SCID mice were treated (day 28) with mMSC-GFP cells administered by either IP or IV routes (**Supplemental Figure 2A**).  Mice were harvested 24 hrs later, and the tumors qualitatively assessed for presence of MSCs by immunofluorescent staining.  Two types of intraperitoneal tumors result in this model: small free floating spheroid tumors and tumors attached to the peritoneal mesentery (2, 32). mMSCs were found in both types of tumors, regardless of tumor size and route of administration, both at the periphery and within the tumor itself (**Figure 2**).  No mMSCs were observed within or along the periphery of the intestines or other abdominal organs (**Supplemental Figure 2B-C**).  There was no obvious macroscopic evidence of tumor metastasis outside of the peritoneal cavity in other organs evaluated including lung, heart, and testes, therefore we did not assess for the presence of MSCs by microscopy in other organs.  Although the number of MSCs that localized to the peritoneal tumors was not quantitated, these results parallel those observed with MSC localization to tumors in a number of other models (22).  Future studies will assess quantitative MSC localization to the inoculated tumors as we further optimize the dose and dosing regimen in this model.

The peritoneal lavage fluid (PLF) was also assessed in these initial localization studies for changes in cytokines and chemokines reflecting the inflammatory microenvironment mediated by innate immune cells present in the SCID mice (**Supplemental Figure 2D**).  IP mMSC administration significantly reduced PLF levels of mouse KC, IL-12(p70), and TNF-α whereas only TNF-α was significantly reduced following IV administration.  Levels of tumor origin human cytokines IL-8, VEGF, and MCAF were decreased following IP mMSC administration, however IV administration had no effect (**Supplemental Figure 2D**).  There was no change in total inflammatory cell numbers

(macrophages, neutrophils, eosinophils) following mMSC administration but a non-significant trend towards an increased percentage of neutrophils was observed in the mMSC treated mice (**Supplemental Figure 2E**).

Even in the limited immune responsiveness context of a Fox Chase SCID mouse, increased inflammation has been closely associated with MM tumor development, with the greatest peritoneal inflammation occurring on days 7 and 14 following tumor inoculation (2, 34).   To assess immunomodulatory effects and any potential effects on tumor burden if MSCs were administered during this period, tumor-inoculated mice received IP administration of mMSCs on days 7 and 14 and were subsequently assessed on day 29 (**Figure 3A**).   A trend towards reduction in mesenteric but not spheroid tumor burden was observed (**Figure 3B**). There was no obvious difference in the overall localization of mesenteric or spheroid tumors within the abdominal cavity. Levels of PLF mouse cytokines were not significantly changed compared to saline treated mice, but a non-significant trend towards decreased levels of human MCAF and VEGF was observed (**Figure 3C**).   There was no significant change in total PLF cell counts but a significant increase in percentage of neutrophils and a decrease in percentage of macrophages were observed, with no differences observed in the eosinophil population (**Figure 3D**).

**TRAIL expressing MSCs induce MM cell apoptosis *in vitro*.**

Human TRAIL protein expression on the mouse MSC cell surface was confirmed by flow cytometry, following transfection, clonal selection, and assessment of differentiation potential (data not shown).  As previously described, treatment of the human MSC-FLT cells with 10μg/mL of DOX for 72 hrs induces TRAIL expression at the cell surface (21).  This expression once induced remains at high levels for an additional 72 hours without further stimulation, before tapering off (21).

Previous microarray analysis of MM lines HMESO and H2373 identified that HMESO cells express TRAIL ligand receptors (Shukla, unpublished data).  Specifically, mRNA was present at

moderate levels for both the apoptosis-inducing death receptors DR4 and DR5 and also the decoy receptor DcR2. Screening the MM cell lines following 24 hour exposure to recombinant human TRAIL protein (rhTRAIL) identified weakly sensitive (HMESO, H2373, HAY) and moderately sensitive (ORT, YOU) MM cells (data not shown). The effectiveness of MSC-TRAIL cells to induce apoptosis was subsequently examined on two selected MM cell lines, HMESO (weakly sensitive) and YOU (moderately sensitive). The MSCs were labeled with a cell tracker dye (CMAC) for these studies and thus the MSC and MM populations were easily distinguished by flow cytometric gating. This allowed determination of the percent of early apoptotic, late apoptotic, and dead MM cells following exposure to MSC-TRAIL cells (**Figure 4A**). Direct co-culture for 24 hrs with MSC-TRAIL cells (either human or mouse), increased the percentage of HMESO and YOU cells that were apoptotic (Annexin-V positive) when compared to control cell lines and positive controls (exposure to 2μg recombinant human TRAIL). HMESO cells were more resistant to hMSC-TRAIL induced apoptosis, just approaching significance (**Figure 4B**), while both clones of mMSC-TRAIL cells induced significant increases in the percent of apoptotic cells (**Figure 4B**). YOU cell apoptosis was significantly increased when cultured with hMSC-TRAIL cells (**Figure 4C**), and also when treated with mMSC-TRAIL clone 87 (clone 49 approached significance) (**Figure 4C**). MSC-Vector cells also increased apoptotic cell number, though not at the significant levels observed in the TRAIL expressing cells, but greater than that in control exposures using recombinant human TRAIL protein itself (**Figures 4B, C**). These data indicate that MSCs alone elicit a modest pro-apoptotic effect, through as yet unclear mechanisms. However, expression of TRAIL further increases apoptosis of the tumor cells.


**Intraperitoneal administration of either mMSC-TRAIL or hMSC-TRAIL significantly decreases peritoneal inflammation, and hMSC-TRAIL further decreases tumor burden.**

Modification of the xenograft model by administering only $1\text{x}10^6$ HMESO cells on day 0 results in a slower tumor development. Starting at 21 days after HMESO inoculation, mice received IP

11

administration of $3x10^5$ mouse or human MSCs, with and without TRAIL expression, twice a week for 3 weeks. Levels of peritoneal inflammation and of tumor burden were subsequently examined at day 46 in comparison to saline-treated controls (**Figure 5A, Supplemental Figure 3A**). mMSC-TRAIL administration (clone 87) had no significant effect on tumor burden (**Supplemental Figure 3B**). There was no change in the percent of different inflammatory cell components within the PLF, however a significant reduction in the PLF total neutrophil count was observed in mMSC-Vector and mMSC-TRAIL treated mice (**Supplemental Figure 3C**). Administration of mMSC-Alone significantly reduced PLF levels of mouse IFN-γ and approached significance in MIP-1α, while mMSC-Vector and mMSC-TRAIL administration significantly reduced MIP-1α but only approached significance in IFNγ (**Supplemental Figure 3D**). A non-significant overall trend toward reduced levels of mouse IL-1rα, IL-2, Eotaxin, KC, MCP-1 (MCAF), and TNFα was observed following administration of mMSC-Alone, mMSC-TRAIL, or mMSC-Vector cells. Significant reductions, compared to saline control, were found in PLF levels of human IL-1rα, IL-1β, IL-15, Basic FGF, GM-CSF, MIP-1α, and RANTES following administration of mMSC-Alone or mMSC-TRAIL (**Supplemental Figure 3E**). Levels of human IL-10 and VEGF exhibited a non-significant trend towards decrease. Administration of mMSC-Vector cells produced similar but non-significant trends towards decrease in levels of these cytokines. No significant changes occurred in human TNF-α for any treatment group. Comparison of mMSC-TRAIL administration to control cell lines mMSC-Alone or mMSC-Vector showed a synergistic effect of the combinatorial MSC+TRAIL administration only in reducing levels of IL-1rα when compared to MSC-Vector (**Supplemental Figure 3E**). Sections of tumor were analyzed for levels of apoptosis by staining for TUNEL. Compared to saline controls in which minimal TUNEL staining was observed, tumors from mice treated with either mMSC-Alone or mMSC-TRAIL cells exhibited increased levels of TUNEL positive cells (**Supplemental Figure 3F**).

In contrast to mMSC-TRAIL, TRAIL-expressing hMSCs significantly reduced tumor burden compared to saline controls (**Figure 5B**). Administration of hMSC-Alone or hMSC-Vector cells also

produced a trend towards reduced tumor burden, but this was not significant compared to saline controls. However, the hMSC effect on tumor burden (either Alone or Vector control) was such that the comparison of MSC-TRAIL to either control group was not additionally significant. hMSC administration (Alone, Vector, and TRAIL) significantly increased the percentage of neutrophils within the PLF cell population (**Figure 5C**) but had no significant effect on the number of total inflammatory cells. Levels of murine CD45 mRNA expression, an index of infiltrating inflammatory cells in the tumors, was not altered in any group examined compared to saline controls (data not shown). Minimal TUNEL staining was observed in saline controls, while in comparison, tumors from mice treated with either hMSC- Alone or hMSC-TRAIL cells exhibited increased levels of TUNEL positive cells (**Figure 5D**), with the greatest levels observed in hMSC-TRAIL treated tumors, indicating that the reduction in tumor burden was correlated with an increase in apoptosis within the tumors.

hMSC administration further significantly decreased levels of multiple PLF cytokines and chemokines, both mouse and human in this model. Administration of hMSCs (all groups) significantly reduced the levels of mouse IL-2, IL-3, IL-10, IL-12(p70) (excluding hMSC-Vector), GM-CSF, MIP-1β, and TNF-α (**Figure 6A**). hMSC-TRAIL treatment also significantly reduced mouse IL-1β, and IL-13, while hMSC-Alone treatment significantly reduced mouse IL-4, and IL-17. Levels of IFN-γ were reduced in every category (hMSC-Alone was not analyzed as only a single data point was above the level of detection) (**Figure 6A**). Comparison of hMSC-TRAIL administration to hMSC-Alone or hMSC-Vector showed a synergistic effect of the combinatorial MSC+TRAIL in reducing levels of mouse GM-CSF, and TNF-α when compared to MSC-Vector, and in TNF-α when compared to MSC-Alone (**Figure 6A**).

Significantly reductions were observed in PLF levels of human IL-1β, IL-10, IL-12(p70), MCP-1(MCAF), RANTES, TNF-α, and VEGF were observed following hMSC-TRAIL administration, while hMSC-Alone and hMSC-Vector had minimal impact (**Figure 6B**). Comparison of hMSC-TRAIL to controls showed that the combinatorial MSC+TRAIL administration was significant in reducing levels

of IL-1β, IL-10, RANTES, and TNF-α when compared to hMSC-Alone. However, the trend towards reduction in hMSC-Vector resulted in no significant differences when compared to hMSC-TRAIL (**Figure 6B**).

In parallel with the earlier studies, hMSC administration resulted in a significant reduction in the PLF mouse and human TNF-α (**Figure 6A, B**), whereas mMSC administration significantly reduced mouse but not human TNF-α in the 24 hr co-localization study (**Supplemental Figure 2D**). The same trend was observed in mouse but not human TNF-α following mMSC administration (**Supplemental Figure 3D, E**).

**Discussion**

Following systemic or intraperitoneal administration, otherwise unmodified mouse or human MSCs could be located in tumors and decreased peritoneal inflammation in an *in vivo* mouse xenograft model of human mesothelioma tumorigenesis. In parallel *in vitro* studies, mouse and human MSCs inhibited migration of multiple MM cell lines following *in vitro* exposure but did not affect other tumorigenic properties. Conversely, conditioned media from MSC/MM cell line Transwell exposure did not significantly alter cytokine release from MM cells, mMSCs, or hMSCs. Administration of mMSCs or hMSCs over-expressing human TRAIL significantly reduced inflammation and while hMSCs alone or transduced with an empty vector produced a trend towards decreased tumor burden, administration of hMSC-TRAIL significantly reduced tumor burden. Administration of mMSCs or hMSCs, regardless of TRAIL expression, increased tumor apoptosis compared to controls. These results suggest a potential role of MSCs and in particular TRAIL-expressing hMSCs in therapeutic approaches for MM.

A rapidly growing literature demonstrates the effectiveness of MSC-based therapy approaches in a variety of pre-clinical inflammatory disease models (35). There are a growing number of clinical trials of MSC therapy in inflammatory and immune based diseases (www.ClinicalTrials.gov), including recent approval for MSC use in severe refractory pediatric graft vs host disease in Canada (36). Importantly, there have been no significant safety concerns or adverse events on follow up in these inflammation-focused trials (37, 38). These findings suggest that MSC-based cell therapy approaches may be particularly appealing for some cancer therapies, though the impact of immunosuppression in cancer and the possible contribution of MSCs to surrounding stroma in some types of cancers (35) will require continued study. Notably MSCs home to areas of both primary and metastatic tumors, through chemotactic pathways still being elucidated (11). MSCs can also alter the tumor microenvironment and decrease inflammation, an important potential therapeutic effect for inflammatory tumors such as MM (39) (40, 41). Other studies have described this innate MSC anti-tumorigenic effect in a number of cancer models (35) thus establishing a potential role for MSCs as non-immunogenic cell based cancer

therapy. Further, a growing literature suggests that engineered MSCs may be even more potent anti-tumor agents. MSCs have been transfected or transduced with recombinant viral vectors to express anti-tumor compounds including Bcl-2 and TRAIL (18-20, 22-25). In particular, recombinant viral transduction of MSCs with human TRAIL has been shown to effectively inhibit *in vivo* progression of lung cancer (22), as well as a variety of primary and metastatic tumors including glioma and breast carcinoma (21, 25), (19). MSC-TRAIL also suppressed proliferation of pancreatic cancer lines *in vitro* (23) and overcame TRAIL resistance in *in vivo* colorectal cancer models (24). Combination of a dodecameric TRAIL vector combined with MSCs engineered to over-express the suicide gene HSV-tk was able to completely inhibit metastatic renal cell carcinoma in a pre-clinical model (20).

With respect to MM, recombinant TRAIL peptides have been demonstrated to induce apoptosis in several MM cell lines (27). A recent study demonstrates that the same TRAIL-expressing hMSCs used in this study were able to reduce tumor burden in a xenograft model of human mesothelioma cells inoculated into the pleural cavity (42) . This study further extends and corroborates those initial findings in a peritoneal model. The current study also includes detailed assessments of MSC effects on the pro-inflammatory peritoneal environment produced in the xenograft model. Our data confirms the induction of MM cell apoptosis observed *in vitro* when treated with MSCs alone or expressing TRAIL (42), and further determines the effects of MSCs alone on MM tumorigenesis using standard *in vitro* assays, aspects which had not previously been assessed in the pleural study.

Acknowledging the limitations of assessing inflammatory pathways in immunocompromised SCID mice, innate immune responses are maintained and there were a number of intriguing findings. Both unmodified and modified MSCs altered the tumor microenvironment through both the reduction in soluble inflammatory mediators, and inducing a shift in the peritoneal inflammatory cell profile. Both of these actions may affect pro- and anti-tumorigenic pathways (43, 44). As MM is a highly inflammatory tumor, and local inflammation is postulated to contribute to both MM survival and proliferation (39, 45), this may be a significant mechanism by which MSC-based therapy could impact

16

clinical MM. As such, these hypothesis-generating observations will be further explored in syngenic immunocompetent allograft models of mouse MM (46). Nonetheless, our findings are in keeping with many observations demonstrating the ability of MSCs to decrease inflammatory tumorogenic environments (11, 13).

We also found that membrane bound human TRAIL-expression on either human or mouse MSCs induced apoptosis in multiple human MM cell lines *in vitro*. Notably, there can be differences in actions of MSCs obtained from mice vs human and soluble anti-inflammatory cytokines released by human MSCs may not be appropriately recognized by murine inflammatory, immune, and other relevant effector cells. Thus, as the overall goal is to develop a strategy for use of human MSCs in mesothelioma, it was important to include both in these initial studies. Importantly, use of human TRAIL-expressing hMSCs in the *in vivo* model resulted in a significant decrease in tumor burden as well as in inflammation. Although hMSCs alone or hMSCs transduced with an empty vector produced trends towards decreased tumor burden, only the TRAIL-expressing hMSCs produced significant decreases compared to saline controls. As treatment with recombinant TRAIL (which has a limited half life around 30 min (42)) did not significantly increase apoptosis *in vitro* (**Figure 4**) we did not include an arm in which recombinant TRAIL peptide alone was administered, but this will be included in future larger scale studies. In some cases synergistic decrease in inflammatory cytokines were observed compared to administration of non-TRAIL expressing MSC controls. In contrast, mouse TRAIL-expressing MSCs decreased inflammation but had no significant effect on tumor burden. The transfected mouse MSCs constitutively express human TRAIL while the transduced human MSCs are induced with DOX, and this induction results in very high expression for 3-4 days, before tapering off. Therefore two doses a week were given to achieve and maintain consistent expression. Identifying whether the potential difference in MSC dose, quantitation of MSC localization to tumor, or species-difference of the MSCs is the key factor in the different results observed will need to be examined in future larger scale studies. Notably, both mouse and human MSCs, regardless of TRAIL expression,

17

stimulated tumor apoptosis but had no significant effects on the number of infiltrating leukocytes. These initial findings will be more extensively explored in future studies, including those in immunocompetent mouse allograft MM models. As these results parallel a number of similar results following administration of MSCs in other cancer models, we did not include an arm with a control (non-MSC) cell line in these initial studies but will do so in future investigations.

Recent data suggests that one potential anti-tumor action of MSCs is through TNF-α signaling. In the context of high levels of NF-κB, TNF-α functions as a pro-survival signal (47), a trait observed in many MM tumor lines (1, 5, 39). Notably, MSC secretion of TSG-6 can inhibit NF-κB signaling (48), while macrophages co-cultured with MSCs exhibited lower TNF-α (49), and TNF-α stimulation of MSCs activated innate TRAIL levels (50). In the current studies, depending on the model utilized both mMSCs and hMSCs suppressed TNF-α levels, MSC-TRAIL treatment synergistically reduced these levels, and the consistent reduction of both mouse and human TNF-α correlated with the reduction in tumor size observed in hMSC-TRAIL therapy. This suggests that inhibition of TNF-α may be a means of breaking the pro-survival signal to allow apoptosis to occur, as seen in the TUNEL staining, and the addition of TRAIL at high levels induces further apoptosis, sufficient to inhibit tumor development. Investigation of TNF-α knockdown in combination with MSC therapy will be a key element of future studies analyzing the mechanism of MSC function.

The 25% reduction in tumor burden observed in the HMESO xenograft MM model, with its high inflammation and only poor-moderate TRAIL-sensitive status, suggests a significant and potentially clinically relevant MSC impact within the constraints of this model. In addition, as inflammation is critical to the pathogenesis, evolution, and maintenance of MM tumors, decrease in inflammatory parameters, even within the constraints of the SCID model utilized suggestive further potential clinical utility of MSC administration in MM (46, 51). Therefore these proof-of-concept studies set the groundwork for more extensive future investigations, while highlighting the potential of MSCs as a potential co-therapy for MM.

## Acknowledgements

## Research Support

## Conflict of Interest

The authors declare no conflict of interest.

**References**

1.      Heintz NH, Janssen-Heininger YM, Mossman BT. Asbestos, lung cancers, and mesotheliomas: from molecular approaches to targeting tumor survival pathways. Am J Respir Cell Mol Biol 2010;42(2):133-9.

2.      Hillegass JM, Shukla A, Lathrop SA, *et al.* Inflammation precedes the development of human malignant mesotheliomas in a SCID mouse xenograft model. Ann N Y Acad Sci 2010;1203:7-14.

3.      Izzi V, Masuelli L, Tresoldi I, Foti C, Modesti A, Bei R. Immunity and malignant mesothelioma: from mesothelial cell damage to tumor development and immune response-based therapies. Cancer letters 2012;322(1):18-34.

4.      Linton A, van Zandwijk N, Reid G, Clarke S, Cao C, Kao S. Inflammation in malignant mesothelioma - friend or foe? Annals of cardiothoracic surgery 2012;1(4):516-22.

5.      Shukla A, Gulumian M, Hei TK, Kamp D, Rahman Q, Mossman BT. Multiple roles of oxidants in the pathogenesis of asbestos-induced diseases. Free Radic Biol Med 2003;34(9):1117-29.

6.      Ray M, Kindler HL. Malignant pleural mesothelioma: an update on biomarkers and treatment. Chest 2009;136(3):888-96.

7.      Sterman DH, Recio A, Haas AR, *et al.* A phase I trial of repeated intrapleural adenoviral-mediated interferon-beta gene transfer for mesothelioma and metastatic pleural effusions. Mol Ther 2010;18(4):852-60.

8.      Prockop DJ, Oh JY. Medical therapies with adult stem/progenitor cells (MSCs): a backward journey from dramatic results in vivo to the cellular and molecular explanations. J Cell Biochem 2012;113(5):1460-9.

9.      Corselli M, Chen CW, Crisan M, Lazzari L, Peault B. Perivascular ancestors of adult multipotent stem cells. Arterioscler Thromb Vasc Biol 2010;30(6):1104-9.

10.     Hodgkinson CP, Gomez JA, Mirotsou M, Dzau VJ. Genetic engineering of mesenchymal stem cells and its application in human disease therapy. Hum Gene Ther 2010;21(11):1513-26.

11.     Hong HS, Kim YH, Son Y. Perspectives on mesenchymal stem cells: tissue repair, immune modulation, and tumor homing. Arch Pharm Res 2012;35(2):201-11.

12.     Keating A. Mesenchymal stromal cells: new directions. Cell Stem Cell 2012;10(6):709-16.

13.     Le Blanc K, Mougiakakos D. Multipotent mesenchymal stromal cells and the innate immune system. Nat Rev Immunol 2012;12(5):383-96.

14.     Peister A, Mellad JA, Larson BL, Hall BM, Gibson LF, Prockop DJ. Adult stem cells from bone marrow (MSCs) isolated from different strains of inbred mice vary in surface epitopes, rates of proliferation, and differentiation potential. Blood 2004;103(5):1662-8.

15.     Prockop DJ, Oh JY. Mesenchymal stem/stromal cells (MSCs): role as guardians of inflammation. Mol Ther 2012;20(1):14-20.

16.     Porada CD, Almeida-Porada G. Mesenchymal stem cells as therapeutics and vehicles for gene and drug delivery. Adv Drug Deliv Rev 2010;62(12):1156-66.

17.     Rebellato LM, Dobbs LJ, Jr. Haploidentical transplantation. Importance of histocompatibility testing and chimerism studies in allogeneic bone marrow/stem cell transplantation. J Infus Nurs 2001;24(5):311-8.

18.     Ciavarella S, Grisendi G, Dominici M, *et al.* In vitro anti-myeloma activity of TRAIL-expressing adipose-derived mesenchymal stem cells. Br J Haematol 2012;157(5):586-98.

19.     Kim SM, Woo JS, Jeong CH, Ryu CH, Lim JY, Jeun SS. Effective combination therapy for malignant glioma with TRAIL-secreting mesenchymal stem cells and lipoxygenase inhibitor MK886. Cancer Res 2012;72(18):4807-17.

20.     Kim SW, Kim SJ, Park SH, *et al.* Complete Regression of Metastatic Renal Cell Carcinoma by Multiple Injections of Engineered Mesenchymal Stem Cells Expressing Dodecameric TRAIL and HSV-TK. Clin Cancer Res 2013;19(2):415-27.

21.     Loebinger MR, Eddaoudi A, Davies D, Janes SM. Mesenchymal stem cell delivery of TRAIL can eliminate metastatic cancer. Cancer Res 2009;69(10):4134-42.

22.    Loebinger MR, Sage EK, Davies D, Janes SM. TRAIL-expressing mesenchymal stem cells kill the putative cancer stem cell population. British journal of cancer 2010;103(11):1692-7.

23.    Moniri MR, Sun XY, Rayat J, *et al.* TRAIL-engineered pancreas-derived mesenchymal stem cells: characterization and cytotoxic effects on pancreatic cancer cells. Cancer Gene Ther 2012;19(9):652-8.

24.    Mueller LP, Luetzkendorf J, Widder M, Nerger K, Caysa H, Mueller T. TRAIL-transduced multipotent mesenchymal stromal cells (TRAIL-MSC) overcome TRAIL resistance in selected CRC cell lines in vitro and in vivo. Cancer Gene Ther 2011;18(4):229-39.

25.    Reagan MR, Seib FP, McMillin DW, *et al.* Stem Cell Implants for Cancer Therapy: TRAIL-Expressing Mesenchymal Stem Cells Target Cancer Cells In Situ. J Breast Cancer 2012;15(3):273-82.

26.    Holoch PA, Griffith TS. TNF-related apoptosis-inducing ligand (TRAIL): a new path to anti-cancer therapies. Eur J Pharmacol 2009;625(1-3):63-72.

27.    Belyanskaya LL, Marti TM, Hopkins-Donaldson S, Kurtz S, Felley-Bosco E, Stahel RA. Human agonistic TRAIL receptor antibodies Mapatumumab and Lexatumumab induce apoptosis in malignant mesothelioma and act synergistically with cisplatin. Mol Cancer 2007;6:66.

28.    Li Q, Verschraegen CF, Mendoza J, Hassan R. Cytotoxic activity of the recombinant anti-mesothelin immunotoxin, SS1(dsFv)PE38, towards tumor cell lines established from ascites of patients with peritoneal mesotheliomas. Anticancer Res 2004;24(3a):1327-35.

29.    Lee RH, Seo MJ, Pulin AA, Gregory CA, Ylostalo J, Prockop DJ. The CD34-like protein PODXL and alpha6-integrin (CD49f) identify early progenitor MSCs with increased clonogenicity and migration to infarcted heart in mice. Blood 2009;113(4):816-26.

30.    Shukla A, Miller JM, Cason C, *et al.* Extracellular signal-regulated kinase 5: a potential therapeutic target for malignant mesotheliomas. Clin Cancer Res;19(8):2071-83.

31.    Toyooka S, Pass HI, Shivapurkar N, *et al.* Aberrant methylation and simian virus 40 tag sequences in malignant mesothelioma. Cancer Res 2001;61(15):5727-30.

32.     Hillegass JM, Blumen SR, Cheng K, *et al.* Increased efficacy of doxorubicin delivered in multifunctional microparticles for mesothelioma therapy. Int J Cancer 2011;129(1):233-44.

33.     Zar JH. Biostatistical analysis. 5th ed. Upper Saddle River, N.J.: Prentice-Hall/Pearson; 2010.

34.     Shukla A, Hillegass JM, MacPherson MB, *et al.* ERK2 is essential for the growth of human epithelioid malignant mesotheliomas. Int J Cancer 2011;129(5):1075-86.

35.     Reagan MR, Kaplan DL. Concise review: Mesenchymal stem cell tumor-homing: detection methods in disease model systems. Stem Cells 2011;29(6):920-7.

36.     Cyranoski D. Canada approves stem cell product. Nat Biotech 2012;30(7):571.

37.     Lalu MM, McIntyre L, Pugliese C, *et al.* Safety of cell therapy with mesenchymal stromal cells (SafeCell): a systematic review and meta-analysis of clinical trials. PLoS One 2012;7(10):e47559.

38.     von Bahr L, Batsis I, Moll G, *et al.* Analysis of tissues following mesenchymal stromal cell therapy in humans indicates limited long-term engraftment and no ectopic tissue formation. Stem Cells 2012;30(7):1575-8.

39.     Jube S, Rivera ZS, Bianchi ME, *et al.* Cancer cell secretion of the DAMP protein HMGB1 supports progression in malignant mesothelioma. Cancer Res 2012;72(13):3290-301.

40.     Ben-Ami E, Berrih-Aknin S, Miller A. Mesenchymal stem cells as an immunomodulatory therapeutic strategy for autoimmune diseases. Autoimmun Rev 2011;10(7):410-5.

41.     Gregory LA, Ricart RA, Patel SA, Lim PK, Rameshwar P. microRNAs, Gap Junctional Intercellular Communication and Mesenchymal Stem Cells in Breast Cancer Metastasis. Curr Cancer Ther Rev 2011;7(3):176-83.

42.     Sage E, Kolluri K, Giangreco A, Janes S. S60 Mesenchymal stem cells expressing TRAIL induce apoptosis in malignant pleural mesothelioma. Thorax 2011;66(Suppl 4):A29.

43.     Hillegass JM, Shukla A, MacPherson MB, *et al.* Mechanisms of oxidative stress and alterations in gene expression by Libby six-mix in human mesothelial cells. Part Fibre Toxicol;7:26.

44.     Liu W, Bodle E, Chen JY, Gao M, Rosen GD, Broaddus VC. Tumor necrosis factor-related apoptosis-inducing ligand and chemotherapy cooperate to induce apoptosis in mesothelioma cell lines. Am J Respir Cell Mol Biol 2001;25(1):111-8.

45.     Liu S, Ginestier C, Ou SJ, *et al.* Breast cancer stem cells are regulated by mesenchymal stem cells through cytokine networks. Cancer Res 2011;71(2):614-24.

46.     Mossman BT, Shukla A, Heintz NH, Verschraegen CF, Thomas A, Hassan R. New insights into understanding the mechanisms, pathogenesis, and management of malignant mesotheliomas. The American journal of pathology 2013;182(4):1065-77.

47.     Fan Y, Dutta J, Gupta N, Fan G, Gelinas C. Regulation of programmed cell death by NF-kappaB and its role in tumorigenesis and therapy. Adv Exp Med Biol 2008;615:223-50.

48.     Choi H, Lee RH, Bazhanov N, Oh JY, Prockop DJ. Anti-inflammatory protein TSG-6 secreted by activated MSCs attenuates zymosan-induced mouse peritonitis by decreasing TLR2/NF-kappaB signaling in resident macrophages. Blood 2011;118(2):330-8.

49.     Kim J, Hematti P. Mesenchymal stem cell-educated macrophages: a novel type of alternatively activated macrophages. Exp Hematol 2009;37(12):1445-53.

50.     Lee RH, Yoon N, Reneau JC, Prockop DJ. Preactivation of human MSCs with TNF-alpha enhances tumor-suppressive activity. Cell Stem Cell 2012;11(6):825-35.

51.     Yan TD, Deraco M, Baratti D, *et al.* Cytoreductive surgery and hyperthermic intraperitoneal chemotherapy for malignant peritoneal mesothelioma: multi-institutional experience. J Clin Oncol 2009;27(36):6237-42.

**Figure Legends**

**Figure 1. MSCs inhibit the tumorigenic properties of malignant mesothelioma cell lines *in vitro*.**

A) Transwell exposure of HMESO or H2373 (Black Circles) cells to either hMSC or mMSC cells (White Squares) did not alter the proliferation profiles over 4 to 7 days. Cell counts are calculated based on independently grown standard curve of MM cells. Experimental replicates=3, data presented as total cell number (mean +/- Std Dev). B) MSCs inhibit the migration capacity of the more migratory MM cell lines – HMESO, H2373, CRL-5820, and CRL-5915, following Transwell exposure to the MSCs for 5 days. N=3, data presented as intensity of crystal violet stain, $OD_{595}$ (mean +/-SEM). C) Invasion across a basement membrane is not affected by 5 days MSC Transwell exposure, n=3, data presented as intensity of crystal violet stain, OD595 (mean +/-SEM). D) Representative images demonstrating that anchorage independent colony formation by HMESO cells is not altered when MSCs are present in the agar, with quantification of live cells by MTT assay. n=3 independent colony formation assay platings. Original Mag 4X. Significance as determined by ANOVA with a Fishers LSD post-test was indicated on each graph as $p \leq 0.05 = *$, $p \leq 0.01 = **$, $p \leq 0.001 = ***$.

**Figure 2. mMSC-GFP cells are present within spheroid and mesenteric tumors at 24 hrs following systemic or localized administration.**

Representative confocal fluorescence microscopy images from 2-4 images scored per tissue, from three mice per injection group. Original Mag 40X, Scale bar indicates 50μm. Arrows indicate MSCs.

**Figure 3. Intraperitoneal administration of mMSCs alter the tumor microenvironment but not the tumor burden.**

A) Schematic of MSC treatment during tumor development experiment protocol. B) Examination of the tumor burden (examined here as the average tumor weight per mouse) in mice treated IP with mMSC cells on day 7 and 14 resulted in a trend toward a reduction in average mesenteric tumor weight. n=7

Saline control (White bars), n=8 MSC IP (Grey bars), data presented as average tumor weight per mouse (mean +/-SEM). C) Bioplex analysis of mouse and human soluble inflammatory cytokines within PLF in the early treatment model identified only a trend in reduction in two human cytokines (MCAF and VEGF). Units are pg/mL (mean +/-SEM). D) Differential cell counts of PLF fluid from the early treatment model identified a significant increase in the percent of neutrophils within the PLF, but no significant change in the PLF total cell count. Percentage or cell count presented (mean +/-SEM). Significance compared to saline control is indicated as $p \leq 0.05$=*, $p \leq 0.01$=**, $p \leq 0.001$=***.

**Figure 4. MSC-TRAIL cells induce apoptosis in MM cell lines *in vitro*.**

A) Flow cytometry schematic. Total cell population was examined by side scatter and Cell Tracker Blue (CMAC - in the DAPI channel). Top two panels: Y-axis – side scatter, X-axis - CMAC fluorescence intensity). CMAC negative cells were examined for Annexin V (PE) (Y-axis) and Viability (7-AAD) (X-axis). Bottom panels: all axis are fluorescence intensity. The percent of Annexin V positive, 7-AAD negative cells was presented as fold change normalized to untreated cells (n=3 experimental replicates, mean +/- SEM). B) HMESO cells cocultured for 24 hrs with MSCs show an increased percent of apoptotic cells. C). YOU cells cultured as above also exhibit increased apoptotic cell numbers. MSC-Vector cell (mouse or human) treatment of either MM cell line results in a modest increase that does not reach significance. Significance as determined by ANOVA with a Fishers LSD post-test, when compared to MM cells alone (untreated) is indicated as $p \leq 0.05$=*, $p \leq 0.01$=**.

**Figure 5. TRAIL-expressing hMSCs inhibit tumor growth when administered intraperitoneally to mature tumors.**

A) Schematic of MSC treatment during tumor development experiment protocol. B) Group average of sum tumor burden per mouse in g (mean +/-SEM). hMSC-TRAIL administration significantly reduced the total weight of tumors, with hMSC-Alone and hMSC-Vector administrations showing modest

reductions. Average tumor burden and the distribution of tumor burden on a per mouse basis are indicated. C) Differential cell populations from within the PLF, data presented as average percent or total cell count (mean +/-SEM). D) Representative images demonstrating positive TUNEL staining of large numbers of tumor cells (yellow-brown) following administration of either mMSC-Alone, hMSC-Alone, mMSC-TRAIL, or hMSC-TRAIL, compared to control. Original magnification 20X, scale bar indicates 200μm. n=5 Saline control, 8 hMSC-Alone, 7 hMSC-Vector, and 8 hMSC-TRAIL. Significance as determined by ANOVA with a Fishers LSD post test, compared to Saline control is indicated as $p \leq 0.05 = *$.


**Figure 6.  hMSC-TRAIL cell therapy alters soluble cytokines of the tumor microenvironment.**

Bioplex analysis of soluble inflammatory cytokines within PLF of mice therapeutically treated with hMSCs identified significant reductions in A) mouse and B) human soluble cytokines.  All units are pg/mL (mean +/-SEM); histogram colors: Saline control: White, mMSC-Alone: Light Grey, mMSC-Vector: Dark Grey, mMSC-TRAIL: Black.   n=5 Saline control, 8 hMSC-Alone, 7 hMSC-Vector, and 8 hMSC-TRAIL.  Significance as determined by ANOVA with a Fishers LSD post-test is indicated as $p \leq 0.05 = *$, $p \leq 0.01 = **$, $p \leq 0.001 = ***$ with respect to saline levels.  Significant changes between hMSC-TRAIL treatment and hMSC-Alone or hMSC-Vector are indicated by the symbols # and @ respectively, and significance is indicated as $p \leq 0.05$ level only.  The addition of p-values approaching significance in the figure represent comparison to saline controls only.

**Supplemental Figure Legends**

**Supplemental Figure 1. MSC effects on MM cell lines shows consistency across multiple cell lines.**

MSC ability to inhibit tumorigenic properties was examined in 11 cell lines, HMESO, H2373, HAY, HEC, ROB, YOU, PET, PRO, ORT, CRL-5820, AND CRL-5915.   A) Initial proliferation characterization of the 7 peritoneal cell lines identified 3 groups with different proliferation ability. Experimental replicates n=3, data presented as cell number (mean +/-Std Dev).  PRO proliferation was so low it was examined for each assay once, and not used for subsequent experimentation.  B) Based on the robust nature (relative to the other 5 peritoneal lines, but still drastically lower than the other 4 lines used) HAY and ORT were tested for the effect of MSC Transwell exposure over days 4-7 of cell growth. n=3, data presented as calculated cell number (mean +/-Std Dev).  C) Migration was examined in all 11 cell lines, with PRO excluded after a single trial.  n=4, data presented as crystal violet intensity by $OD_{595}$ (mean +/-SEM) normalized to an equally stained, empty Transwell background level. D) Invasion was examined in all cell lines once, and repeated in HMESO H2373, CRL-5820, CRL-5915, HAY, HEC, ROB, YOU and ORT.  n=4 data presented as crystal violet intensity by $OD_{595}$ (mean +/-SEM) normalized to an equally stained, empty Transwell background level. E) Bioplex analysis of MSC cytokine expression in Transwell culture supernatants at day 6.  Clusters of three bars are colored per MM cell line exposed to, in all cases the left bar is levels produced by MM cell line alone, the center bar (over label tick mark) indicates hMSC Transwell exposure (cytokines produced by both MM and hMSC cells), and the right bar indicates mMSC Transwell exposure. All units are pg/ml (mean +/- SEM). Significance as determined by ANOVA with a Fishers LSD post test, in comparison to medium alone is indicated as $p \leq 0.05 = *$, $p \leq 0.01 = **$, $p \leq 0.001 = ***$.


**Supplemental Figure 2.  MSCs alter the tumor microenvironment and MSCs localize to the site of MM tumor growth and are not observed on intestines at 24 hrs.**

**Effects of TRAIL-Expressing MSCs on Mesothelioma**

A) Schematic of localization experiment protocol.  B) mMSC-GFP cells are not observed in intestinal tissues from tumor bearing mice (n=3 mice per group, tumor and intestine blocks).  Staining of paraffin embedded sections using an anti-GFP-Alexa-555 conjugated antibody, following antigen retrieval. Staining controls from a WT C57Bl6 mouse, and a ubiquitous GFP (C57Bl6 CMV-GFP) mouse were used to identify antibody specificity and function. Auto-fluorescence in the red channel (arrows) was observed in the enterochromaffin cells in all intestines examined.  GFP fluorescence was never observed to co-localize with the auto-fluorescence of the enterochromaffin cells.  The tissue section of WT gut shown was proximal to inner surface so none is seen in this image.  Overlap of the Alexa-555 and GFP fluorescence is considered positive for mMSC-GFP cells.  Intestine sections from mice treated IV with mMSC-GFP cells identified no positive staining for MSC cells, as shown here (bracket) nor in any region examined.  The interior of mesenteric tumors of IV treated mice showed the presence of mMSC-GFP cells (Arrows).  All original magnification: 20X.  C) Examination of additional IV treated mouse intestinal sections identified no positive mMSC-GFP staining, nor in any region examined.  In contrast, examination of mesenteric tumor sections identified mMSC-GFP cells within the interior of the tumors (images 1-4) and along the periphery (4) (Arrows).  All original Mag 20X.  Similar levels of mMSC-GFP cells were observed in IP injection tumor sections, and again, no MSCs were ever observed in IP mouse intestine samples.  Representative images are shown. D) Bioplex analysis of mouse and human soluble inflammatory cytokines in PLF identified significant alterations in the tumor microenvironment at 24 hrs.  All units are pg/mL (mean +/- SEM). E) Differential cell population analysis at 24 hrs post MSC administration displayed as percentages cells within the PLF, and as total cell number, as determined by three independent counts averaged per group (mean +/-SEM).  n=5 control, 5 MSC IV, and 5 MSC IP animals.  Significance, determined by ANOVA with a Fishers LSD post test, using comparison to saline control is indicated as $p \leq 0.05 = *$, $p \leq 0.01 = **$.

**Supplemental Figure 3. TRAIL-expressing mMSCs alter the soluble cytokines of the tumor microenvironment and induce apoptosis, but have no effect on tumor growth when administered intraperitoneally to mature tumors.**

A) Schematic of MSC cell therapy experiment protocol. B) Average sum tumor burden and the distribution of sum tumor burden on a per mouse basis are indicated (mean +/-SEM). C) Differential cell populations from within the PLF are presented as percentages of cells within the population, and total cell number in PLF (mean +/-SEM). D) Bioplex analysis of soluble inflammatory cytokines within PLF of mice therapeutically treated with mMSCs identified significant reductions in D) mouse and E) human soluble cytokines. All units are pg/mL (mean +/-SEM); histogram colors: Saline control: White, mMSC-Alone: Light Grey, mMSC-Vector: Dark Grey, mMSC-TRAIL: Black. F) Representative images demonstrating positive TUNEL staining of large numbers of tumor cells (yellow-brown) following administration of either mMSC-Alone or mMSC-TRAIL, compared to control. Original magnification 20X, scale bar indicates 200μm. n=5 Saline control, 7 mMSC-Alone, 8 mMSC-Vector, and 6 mMSC-TRAIL. Significance as determined by ANOVA with a Fishers LSD post test is indicated as $p \leq 0.05$=\*, $p \leq 0.01$=\*\*, $p \leq 0.001$=\*\*\* with respect to Saline levels. Significant changes between mMSC-TRAIL treatment and mMSC-Alone or mMSC-Vector are indicated by the symbols # and @ respectively, and significance is indicated as $p \leq 0.05$ level only. The addition of p-values approaching significance in the figure represent comparison to Saline controls only.

# Figure 1

# Figure 1

C

### HMESO



### CRL-5820



D

## Colony Formation

| hMSC | HMESO | HMESO:hMSC |
|------|-------|------------|
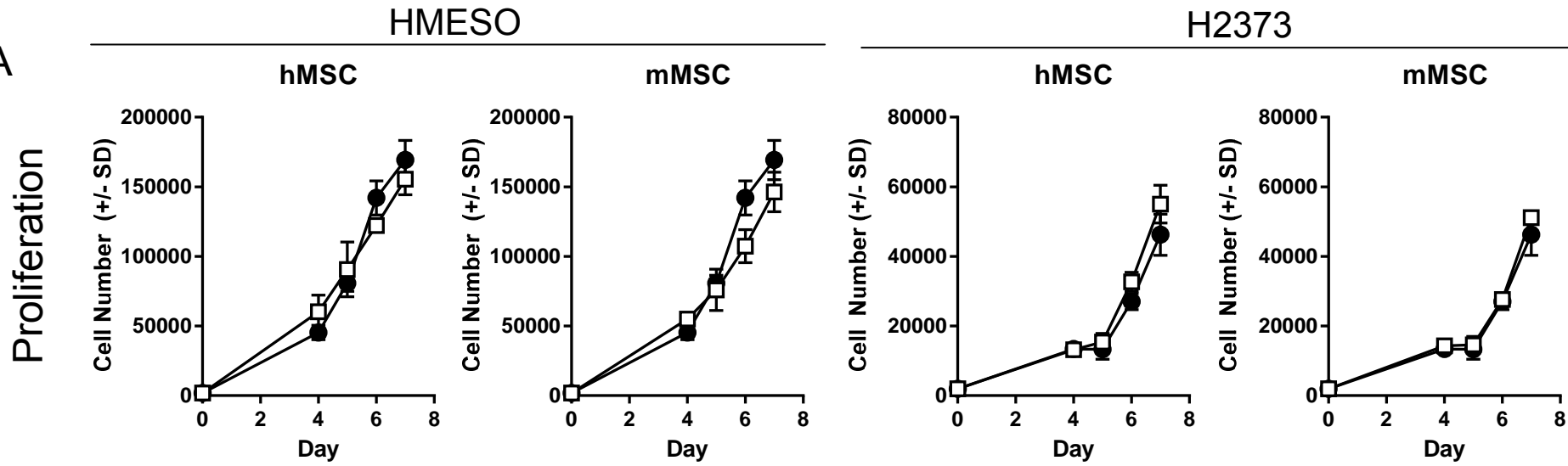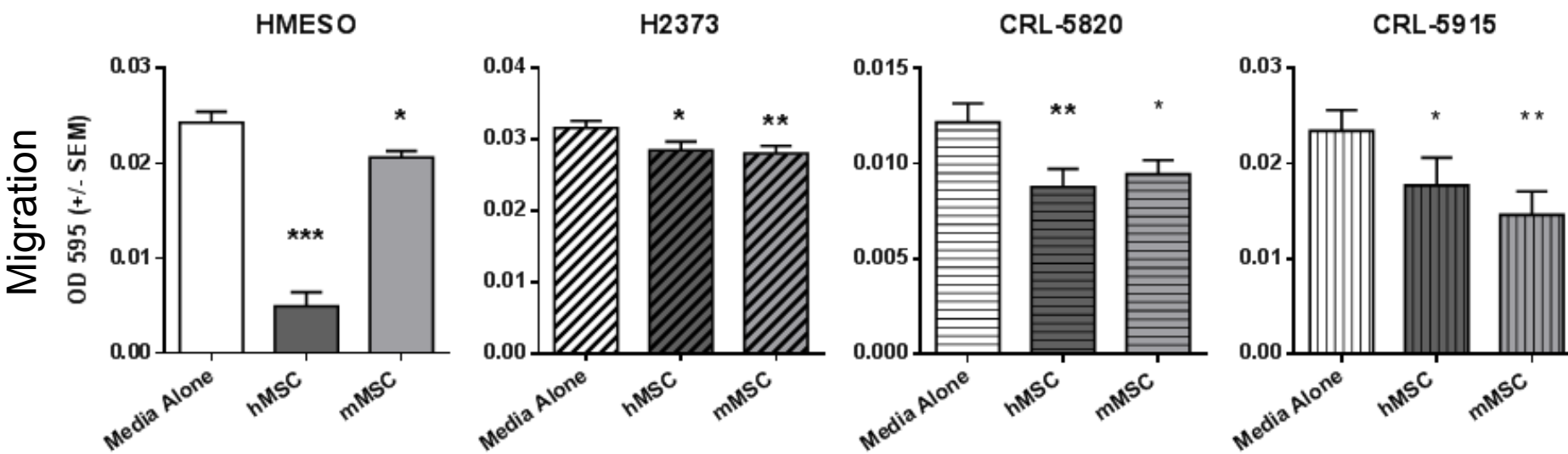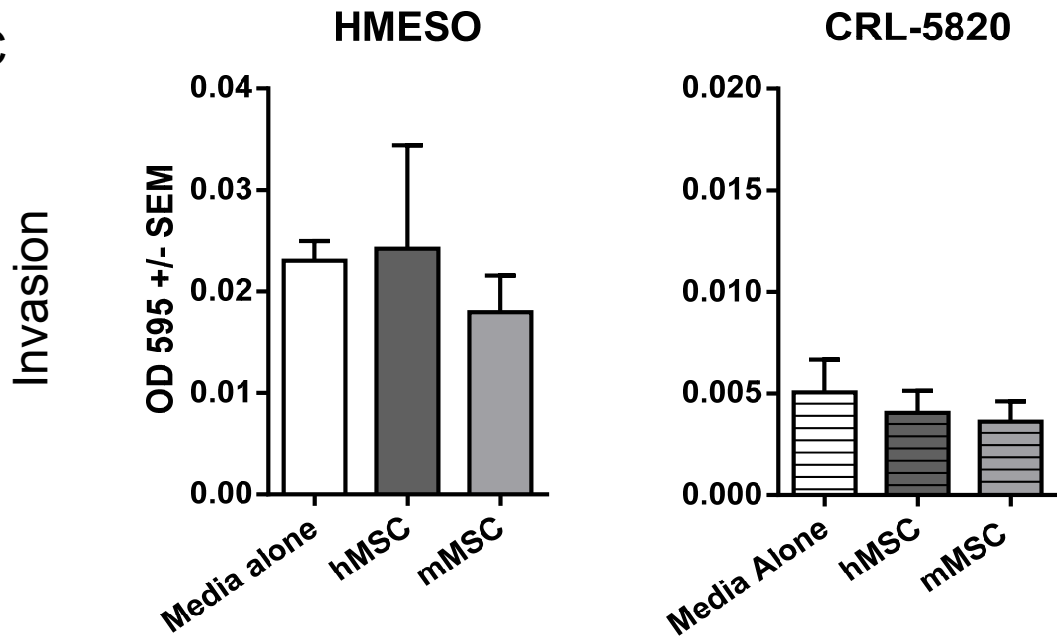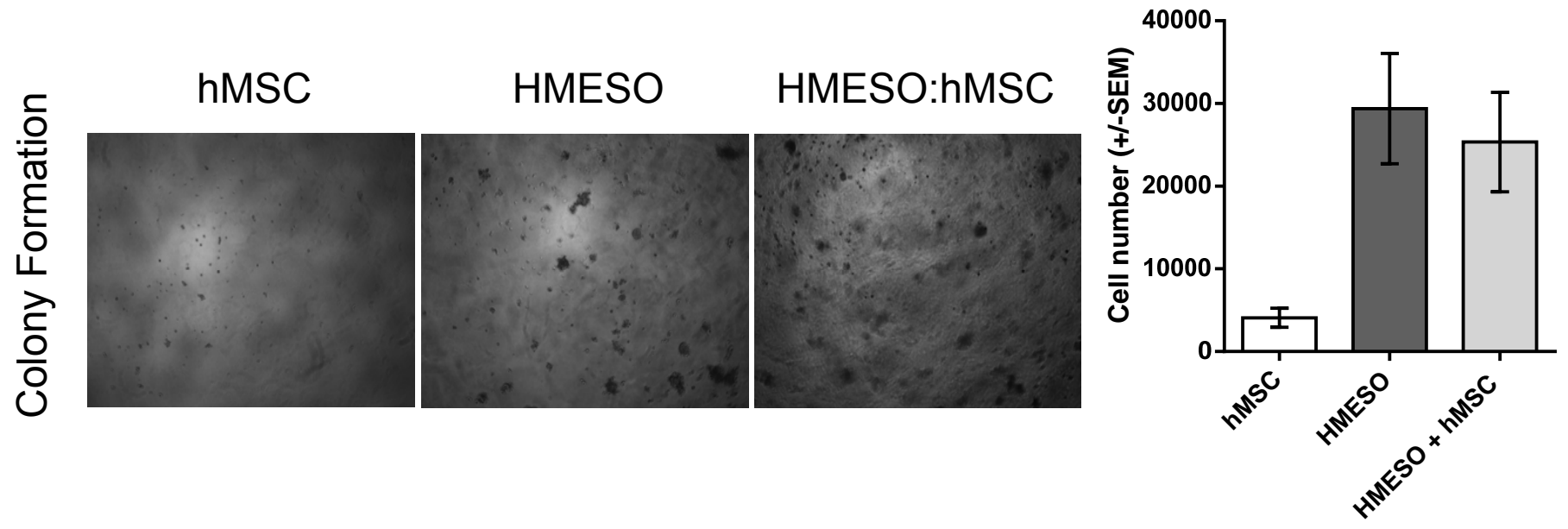
Figure 2
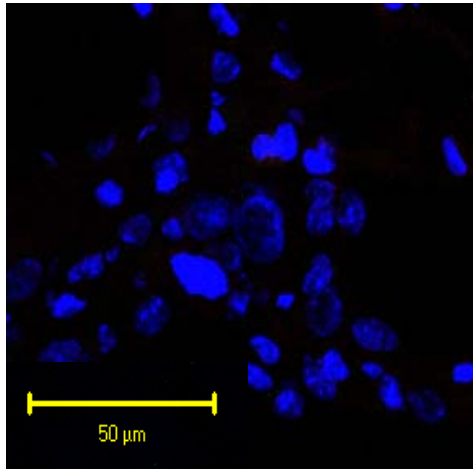


Saline Control          IP/ Mesenteric          IV/ Mesenteric

50 μm                   50 μm                   50 μm

IP/ Spheroid            IV/ Spheroid

50 μm                   50 μm

# Figure 3

## A

HMESO

mMSC

$5 \times 10^6$

$1 \times 10^6$ IP

+

Day 0    7    14    29

Endpoints

Tumor Burden
Tumor Microenvironment
-Inflammatory cytokines
-Cell population

## B



Grams (+/- SEM)

p=0.20

p=0.16

Spheroid    Mesenteric    MSC Spheroid    MSC Mesenteric

## C



MCAF

p=0.35

Control    MSC

VEGF

p=0.15

Control    MSC

## D



Percent of cells (+/- SEM)

**

**

Macrophage    Neutrophil    Eosinophil    Lymphocyte

Total Cell Number (+/- SEM)

Macrophage    Neutrophil    Eosinophil    Lymphocyte

# Figure 4

Figure 5

A

HMESO

1x10^6

MSC-Alone
MSC-Vector
MSC-TRAIL

3x10^5 IP

Endpoints

Tumor Burden
Tumor Microenvironment
  -Inflammatory cytokines
  -Cell population

Day 0    7    14    21    28    35    42  46

B

hMSC Therapy

C

# Figure 5

## D

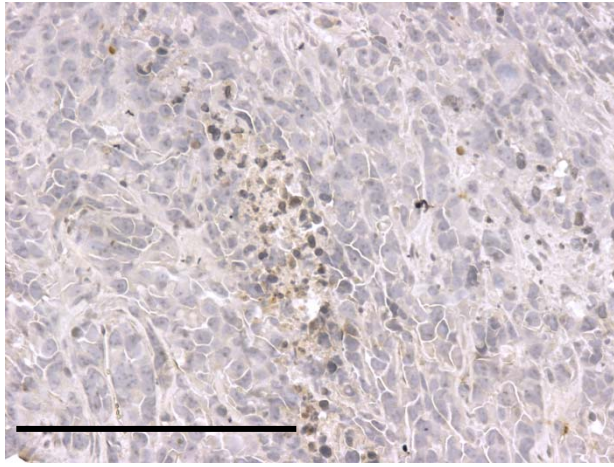| Saline Control | hMSC-Alone | hMSC-TRAIL |
| --- | --- | --- |
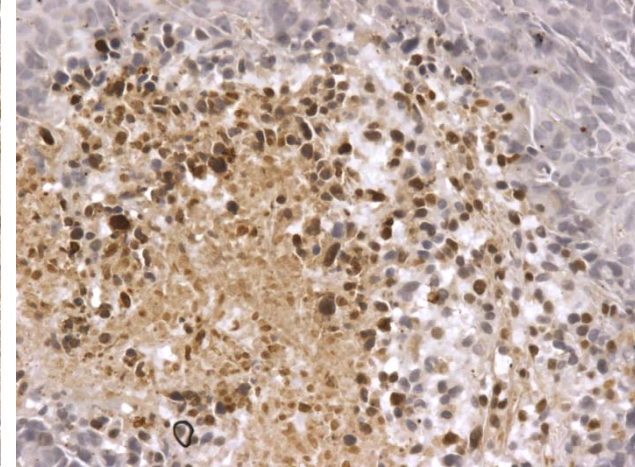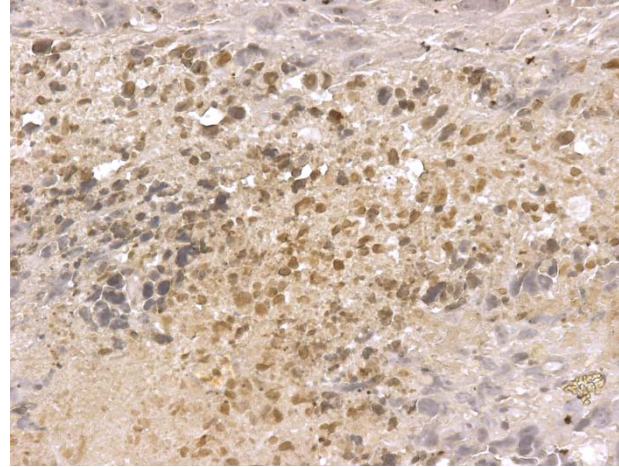
# Figure 6

# Mouse Cytokines

A
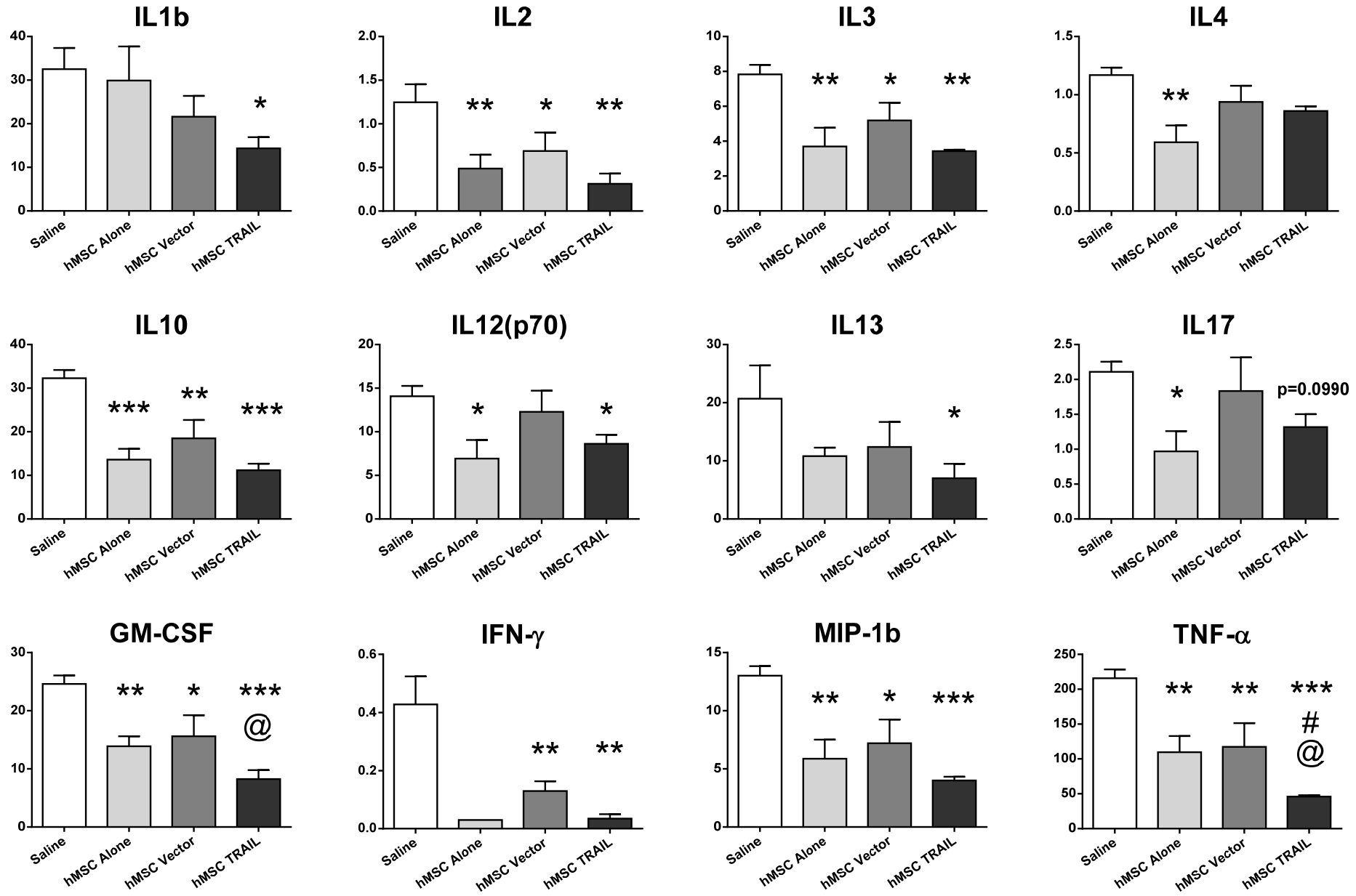
# Figure 6

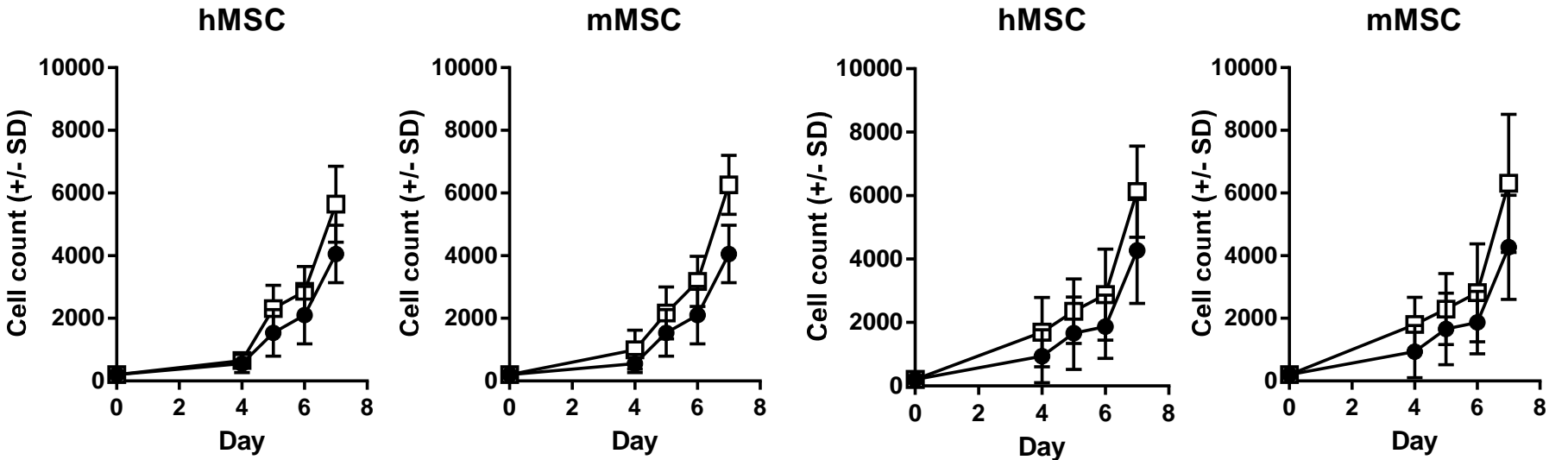## Human Cytokines

B



**IL1ra**

p=0.0588

Saline   hMSC Alone   hMSC Vector   hMSC TRAIL

**IL1b**

\*
#

Saline   hMSC Alone   hMSC Vector   hMSC TRAIL

**IL10**

\*
#

Saline   hMSC Alone   hMSC Vector   hMSC TRAIL

**IL12(p70)**

\*

Saline   hMSC Alone   hMSC Vector   hMSC TRAIL

**MCP-1 (MCAF)**

p=0.0637

\*

Saline   hMSC Alone   hMSC Vector   hMSC TRAIL

**RANTES**

\*
#

Saline   hMSC Alone   hMSC Vector   hMSC TRAIL

**TNF-α**

\*   \*\*
#

Saline   hMSC Alone   hMSC Vector   hMSC TRAIL

**VEGF**

\*

Saline   hMSC Alone   hMSC Vector   hMSC TRAIL

# Supplemental Figure 1

## A   Proliferation



## B

# Supplemental Figure 1

## C  Migration

Supplemental Figure 1

D    Invasion

Supplemental Figure 1

E

# Supplemental Figure 2

A

HMESO

mMSC-GFP

Endpoints

5x10$^6$

1x10$^6$ IP or IV

MSC Localization
Tumor Microenvironment
   -Inflammatory cytokines
   -Cell population

Day 0

28   29

# Supplemental Figure 2

B

|  | Dapi | GFP | Anti- GFP Alexa 555 | Merged |
|---|---|---|---|---|

**WT Intestine Negative ctrl**

**GFP Intestine Positive Control**

**mMSC-GFP treated IV injection**

**Intestine**

**Mesenteric Tumor**

Supplemental Figure 2

C

| | | Dapi | GFP | Anti- GFP Alexa 555 | Merged |
|---|---|---|---|---|---|

**mMSC-GFP treated IV injection Intestine**

**Mesenteric Tumors**

1

2

3

4

# Supplemental Figure 2

# Supplemental Figure 3

Supplemental Figure 3

Mouse Cytokines
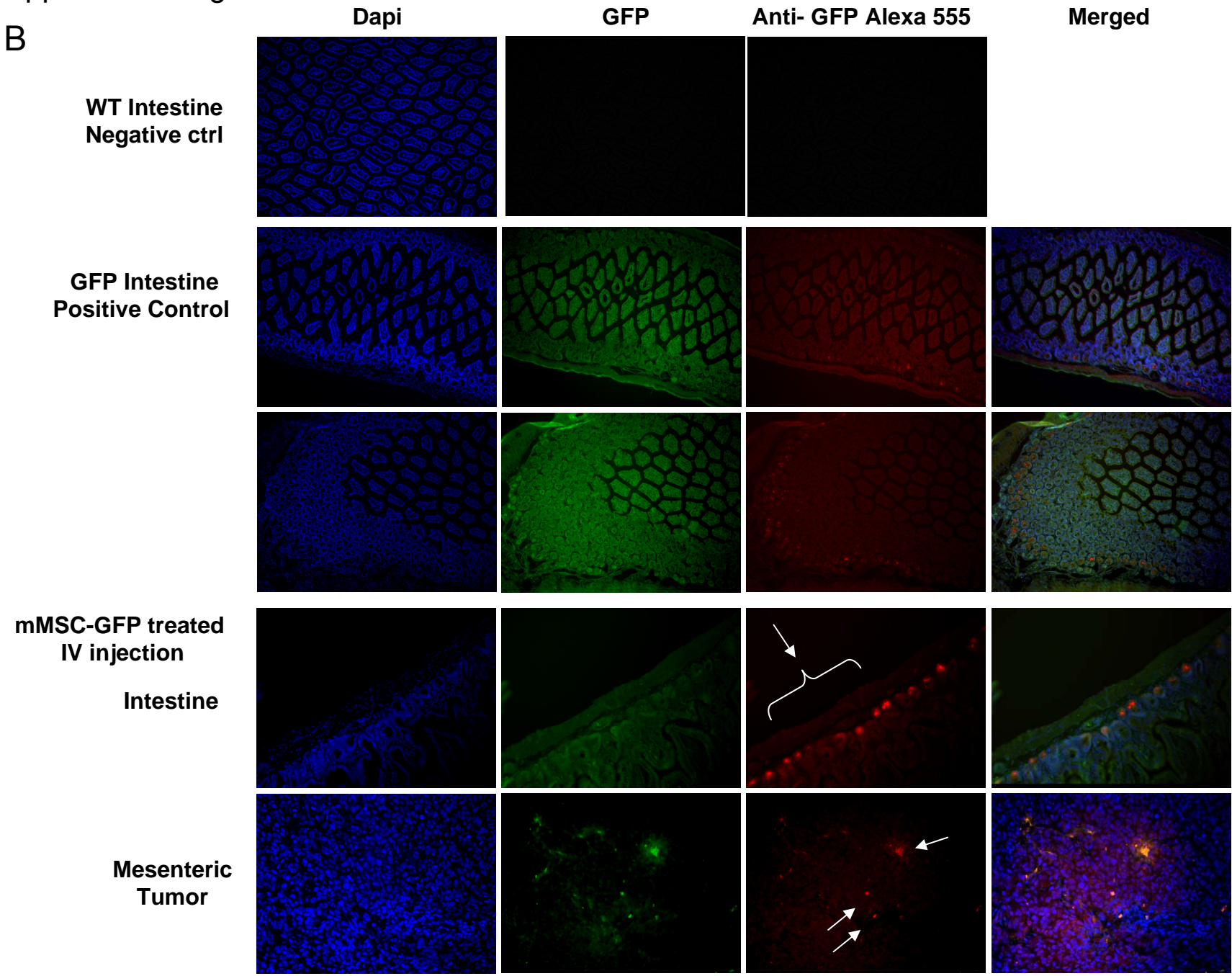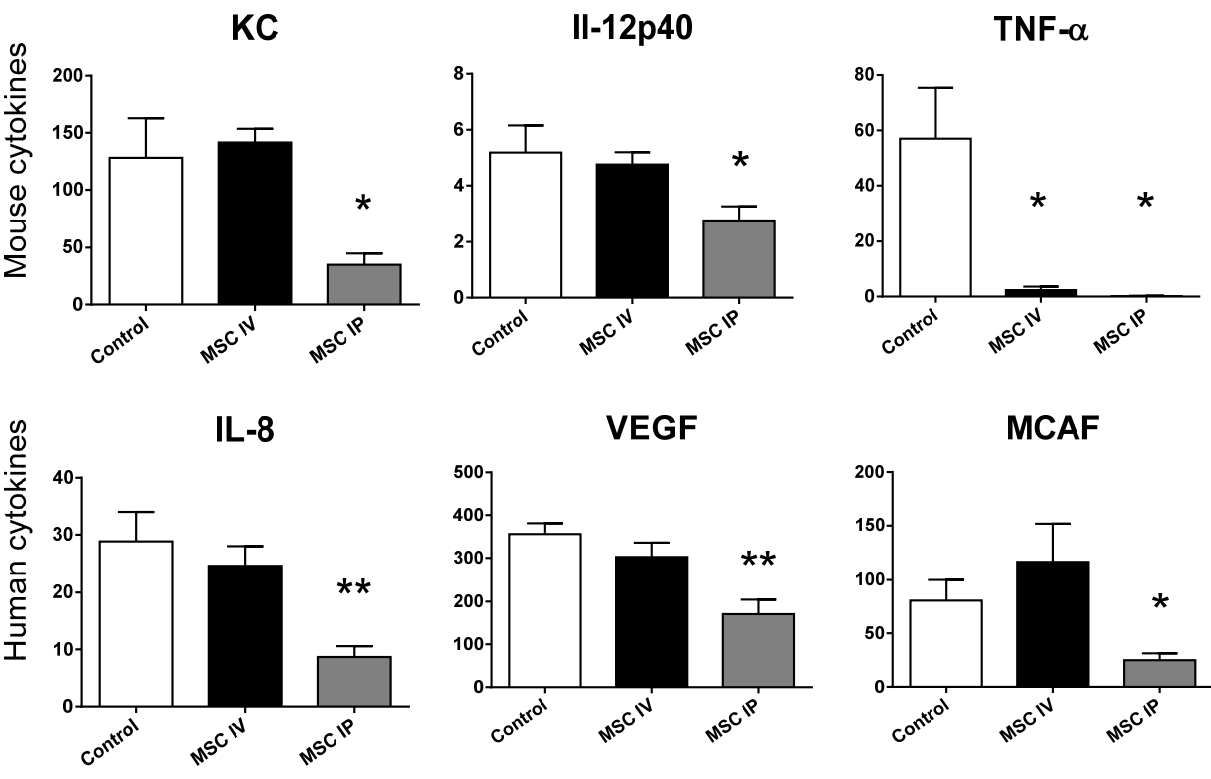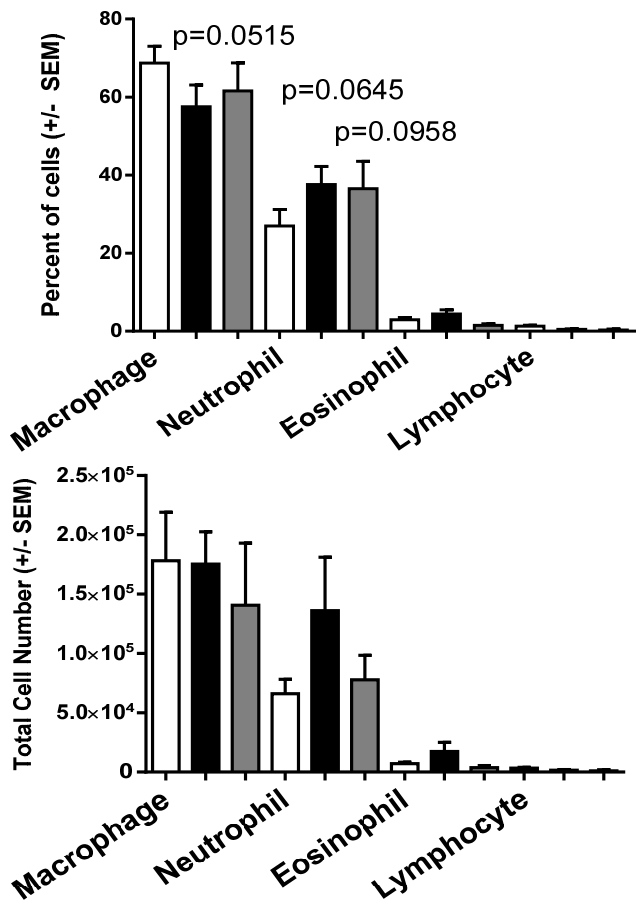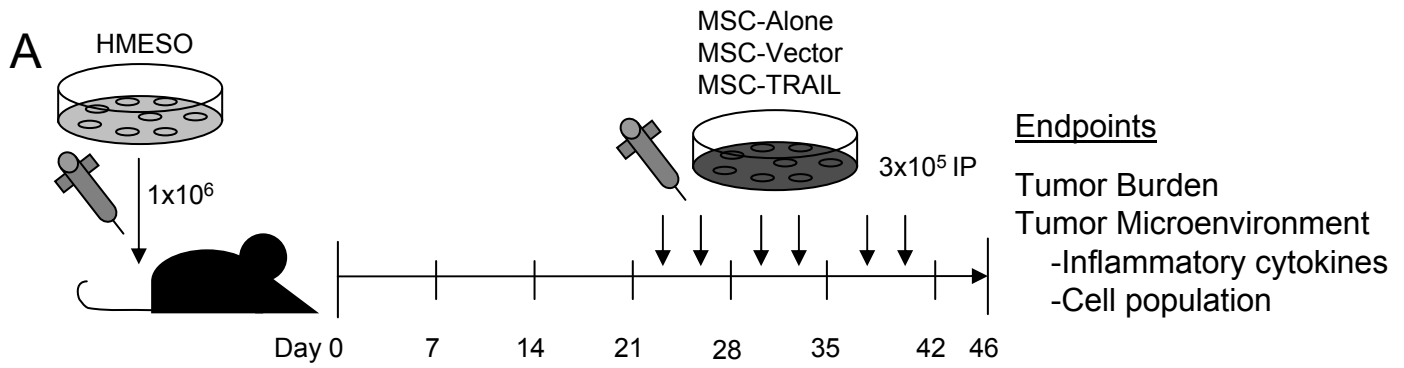
D
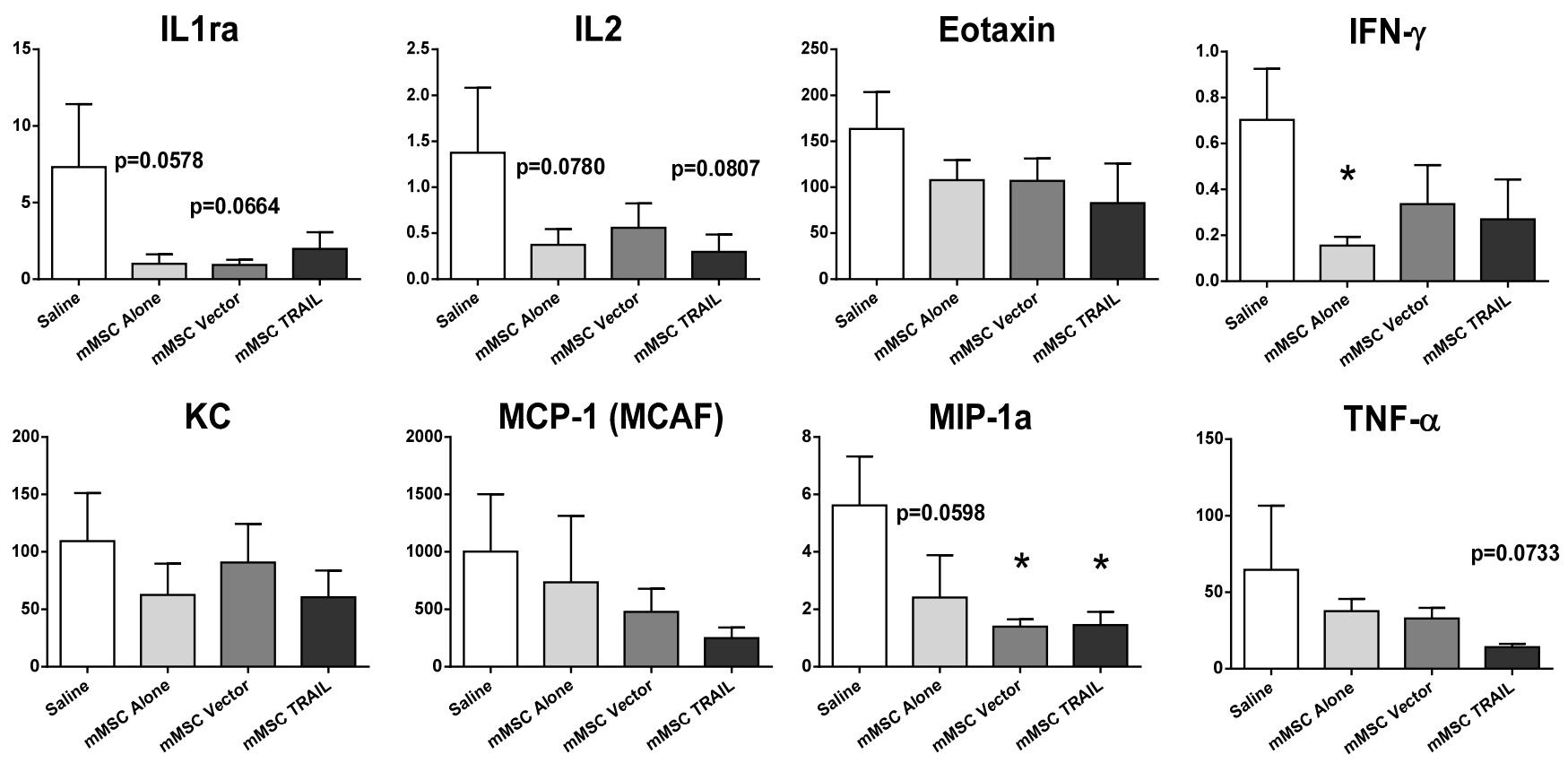
# Human Cytokines

E

# Supplemental Figure 3

## F
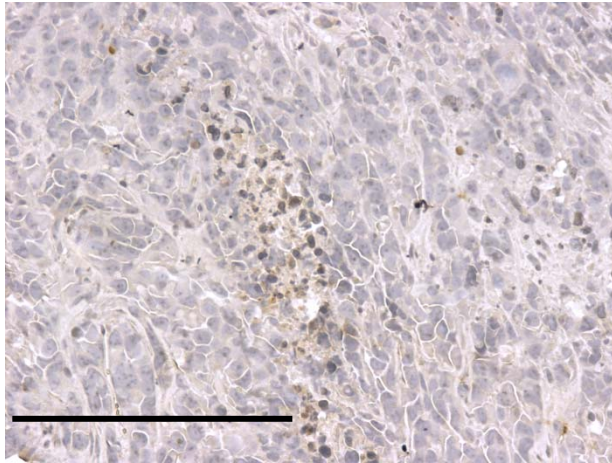
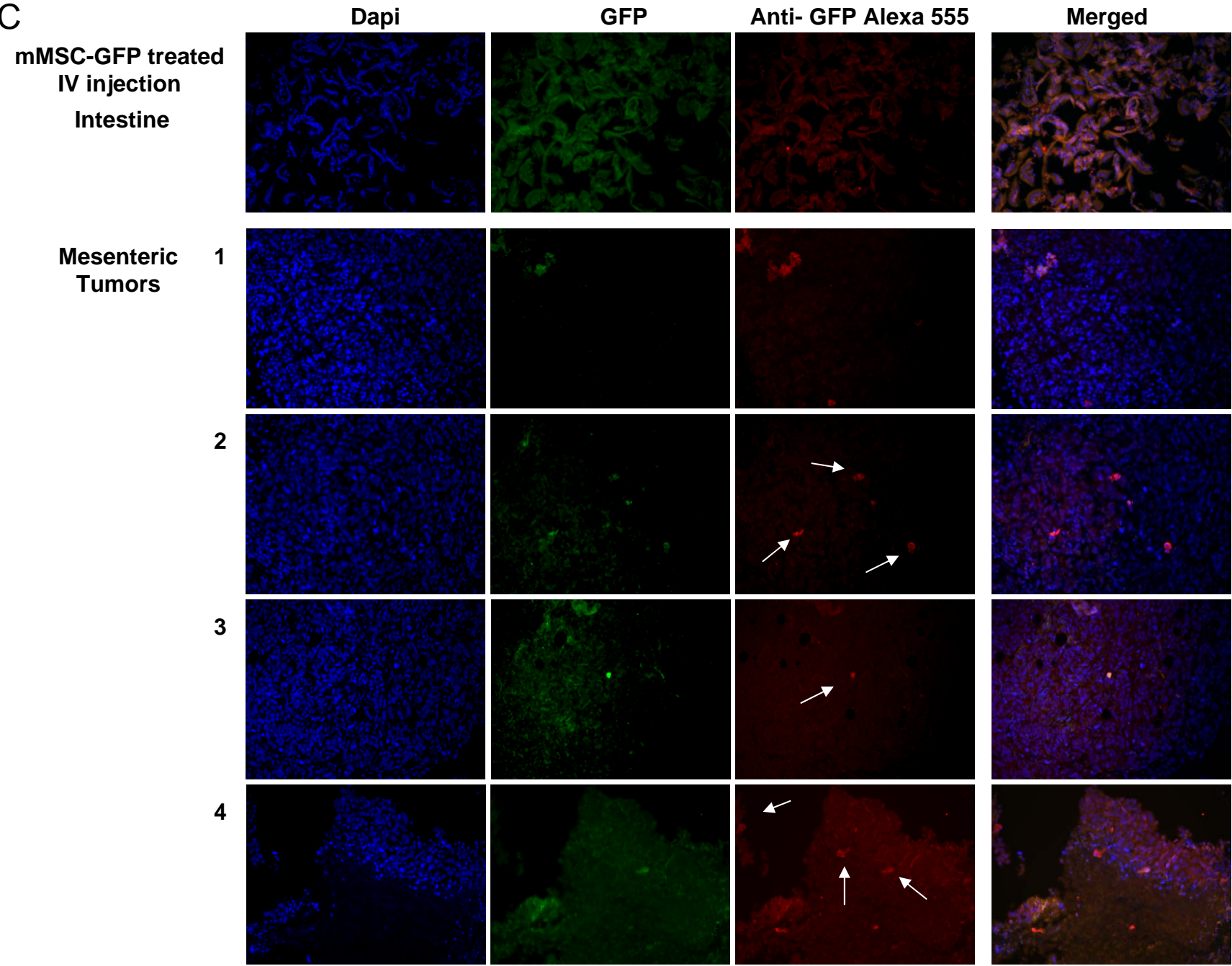| Saline Control | mMSC | mMSC-TRAIL |
|:---:|:---:|:---:|
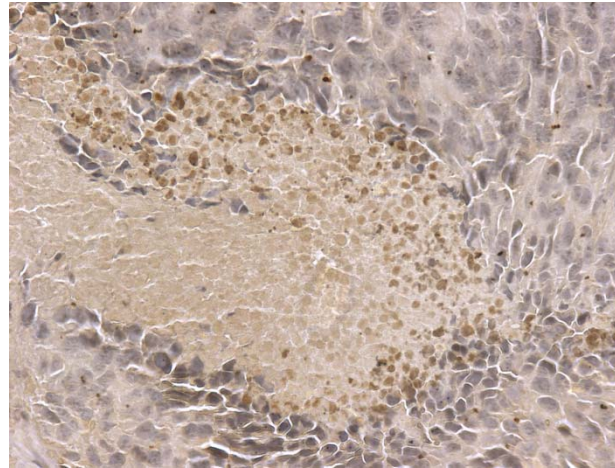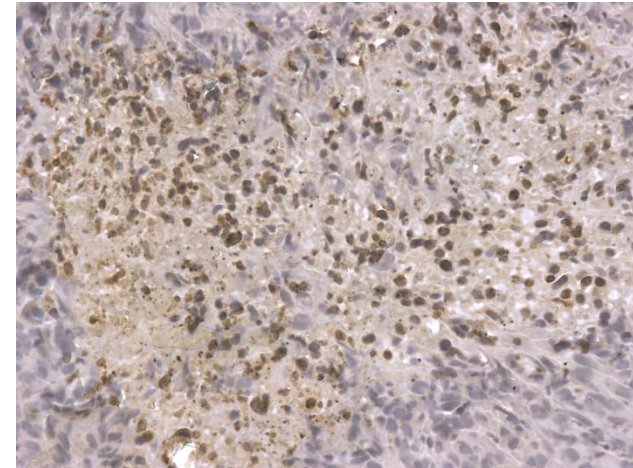


200μm

Note: saline control image is the same for both groups as images were taken at the same time

## Supplemental Methods:

### Cell culture

Murine Mesenchymal Stromal Cells (mMSCs) at passage 3 and 5 were obtained from the Texas A&M Stem Cell Core facility. These cells have previously been extensively characterized for cell surface marker expression and differentiation capacity. Bone marrow MSCs from C57Bl/6J (mMSC) and C57BL/6-Tg(UBC-GFP)30Scha/J mice (GFP-mMSCs) were purchased. Cells were expanded in culture using *mMSC media*: Isocove's Modification of Dulbecco's Medium (IMDM) (Gibco, Life Technologies Grand Isle, NY), 10% Horse Serum (Hyclone, Rockford, IL), 10% fetal bovine serum (FBS) (Hyclone, Rockford, IL), 50 U/ml penicillin G/50 µg/ml streptomycin sulfate (1%) (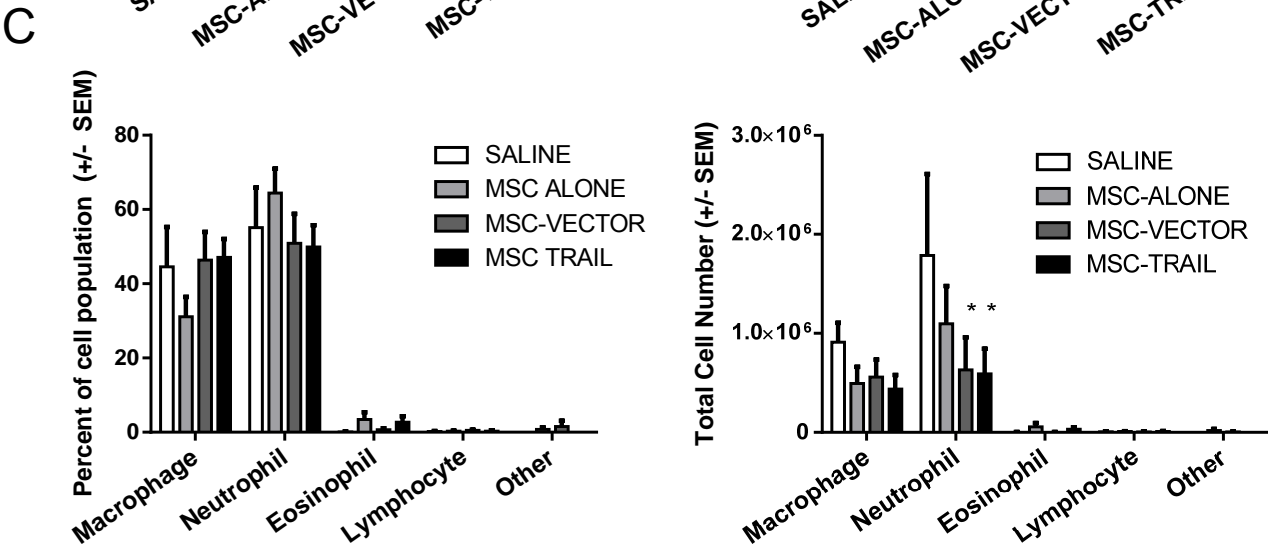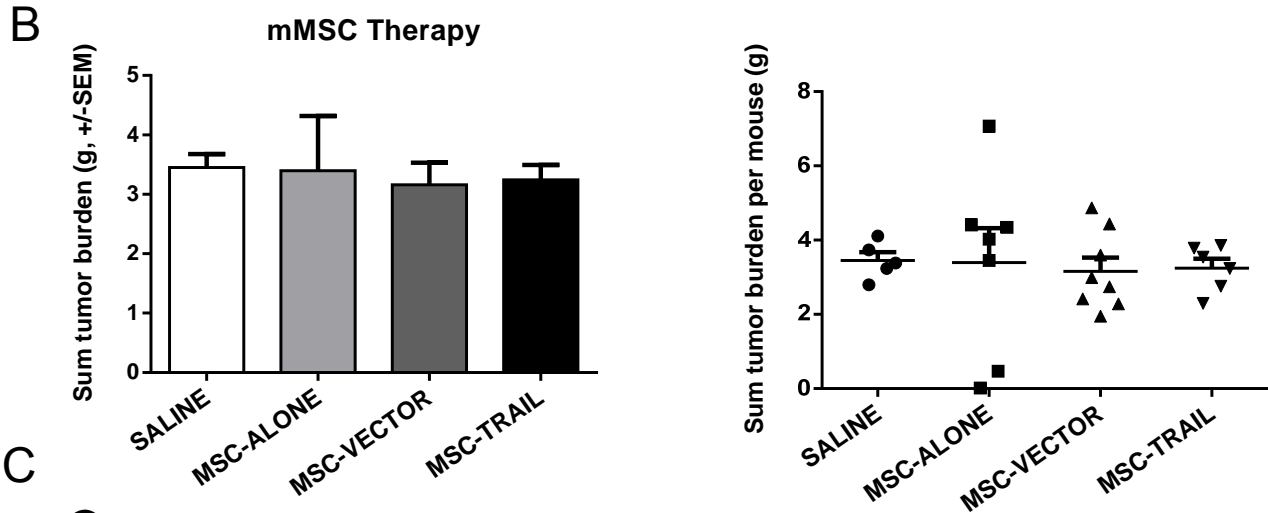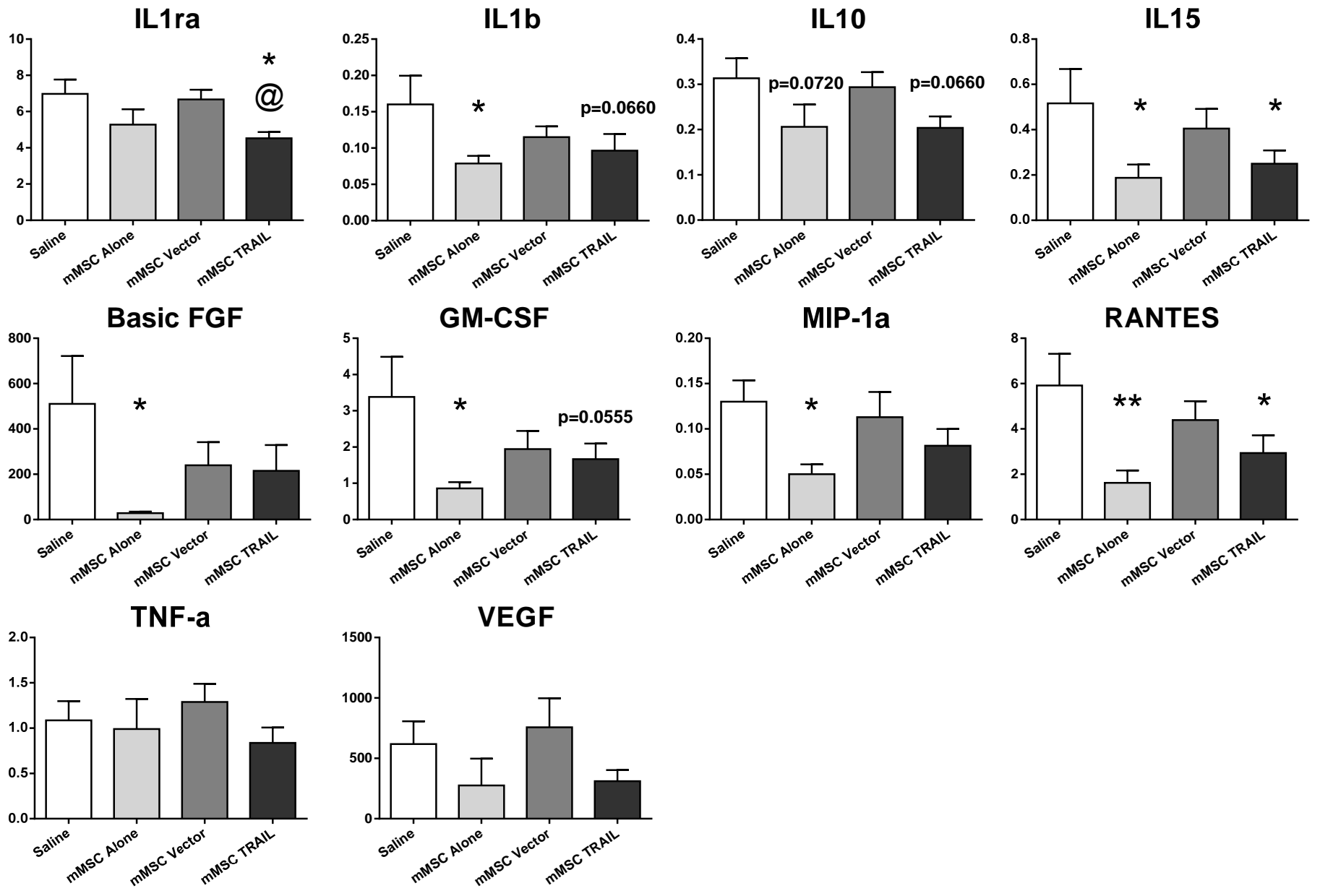Pen/Strep) (Invitrogen, Life Technologies Grand Isle, NY), 2mM L-glutamine (1X) (L-Glut) (Invitrogen, Life Technologies Grand Isle, NY), and used at passages 7-8. Cells were trypsinized for injection using 2.5% Trypsin/EDTA (Invitrogen, Life Technologies Grand Isle, NY), counted using a hemacytometer, and re-suspended in 1X phosphate-buffered saline (PBS), to a final concentration of $1x10^6$ cells per 300µl. An aliquot of the same PBS was made for injection of control mice. mMSCs at passage 3 were cultured as described above, and used for stable transfection and G418 clonal selection and expansion of hTRAIL plasmid (Truclone plasmid SC126304, Origene)

Human Mesenchymal Stromal Cells (hMSCs) at passage 5 were obtained from the Texas A&M Stem Cell Core facility. Bone marrow human MSCs (hMSC) were expanded and lentivirus transduced with green fluorescent protein (GFP). All human MSCs used in the *in vitro* experiments described here expressed cytoplasmic GFP. Cells were expanded in culture using *hMSC media*: Modification of Eagle Medium-Earls Balanced Salt Solution (MEM-EBSS) (Hyclone), 20% FBS, 1% Pen/Strep, 2mM L-Glut, and used at passages 7-8. Cells were expanded, and trypsinized for injections as described above.

Human bone marrow MSCs which were transduced with TRAIL were provided to Dr. Sam Janes by Dr Mark Lowdell (Paul O'Gorman Laboratory of Cellular Therapeutics, Royal Free Hospital,

London, UK), and were cultured as described for hMSCs above. MSCs transduced with a Tet-on plasmid had FBS replaced with Tet-system approved FBS (Clontech, Paris, France).

A549 cells are available commercially from ATCC, and were cultured in *MM media*: Dulbecco's Modified Eagle Medium: Hams F-12 (DMEM:F12) 50:50 mix (Hyclone, Rockford, IL), 10% FBS, 1% Pen/Strep, 2mM L-Glut. Cells were grown until 80% confluent, lifted as described previously and pelleted for RNA isolation.

Jurkat cells are available commercially from ATCC and were cultured in RPMI, 5% FBS, 1X Pen/Strep, 2mM L-glut, 2500mg/ml Glucose, 1mg/ml Folate in 2g/L Sodium Bicarbonate, 1mM Sodium Pyruvate, and 50µM Beta-mercaptoethanol. Cells were cultured and treated with recombinant human TRAIL protein as the positive control for apoptosis induction.

## MM cell lines

Human pleural mesothelioma cell lines Hmeso and PPM Mills were provided by the Mossman lab. The Hmeso cell line was previously described (2) and obtained from Dr. Joseph Testa (Fox Chase Cancer Center, Philadelphia PA). The PPM Mill line (H2373) was previously isolated by Dr. Harvey Pass, (NYU Langone Medical Center) (2). Cells were expanded in culture using *MM media + HITS*: Cells were expanded in culture using MM medium consisting of Dulbecco's Modified Eagle Medium: Hams F-12 (DMEM:F12) 50:50 mix (Hyclone, Rockford, IL), 10% fetal bovine serum (FBS) (Hyclone), 50U/mL penicillin G/50µg/mL streptomycin sulfate (1%) (Pen/Strep) (Invitrogen, Grand Isle, NY), 2mM L-glutamine (L-Glut) (Invitrogen), and 0.1µg/mL hydrocortisone, 2.5µg/mL insulin, 2.5µg/mL transferrin, 2.5ng/mL sodium selenite (HITS) (Sigma Aldrich, St. Louis, MO).

Human peritoneal MM cell lines HAY, YOU, ROB, ORT, PET, PRO, and HEC cell were isolated by Dr. Claire Verschraegen (The University of New Mexico Health Science Center - Cancer Research and Treatment Center), were previously described (28), and were generously provided by the

Verschraegen lab. Human pleural MM cell lines CRL-5820 and CRL-5915 are commercially available cell lines from American Type Culture Collection (ATCC), described further in Toyooka (31), and generously provided from the Janes Lab. These nine cell lines were cultured using MM media.

## Co-culture of MM cells and MSCs

MM cell lines and MSC cell lines were trypsinized off of the plate using 2.5% Trypsin/EDTA (Invitrogen), counted using a hemacytometer, and were plated in each media (hMSC media, mMSC media, MM media and MM media +HITS) alone to determine viability. Adherence to tissue culture dishes at 24 hrs and proliferation by 72 hrs was considered viable. MSC cells are adherent and viable in MM media and MM media +HITS, and all MM cell lines were adherent and viable in hMSC media, however 6 of the 11 MM cell lines were not adherent in mMSC media. The non-adherent cells were examined for viability using trypan blue exclusion, and cell count on hemacytometer, which determined that the MM cells were still live, but not proliferating in the mMSC media, as a loss of cell number relative to the initial plated count was always observed. Therefore further *in vitro* experiments were performed in either MM media or MM Media +HITS as determined by the MM cell line in use.

GFP-mMSCs were plated at an equal number with Hmeso cells in the same well of a 6-well dish using MM media +HITS, and examined by light and fluorescence microscopy on day 2 for adherence to confirm that both cell lines would adhere for co-culture analysis. Hmeso and GFP-mMSC or hMSCs co-cultures were allowed to grow until day 7 and the all cells were examined for proliferation by microscopy, and by flow cytometry gated for GFP. Flow cytometric analysis of these populations for the overall ratio of MSC to Hmeso cell numbers revealed that the cells maintain the ratio that they were plated at (data not shown), and that this held true for both mouse and human MSCs.

**hTRAIL transfection, transduction, and induction**

Mouse bone marrow-derived MSCs were transfected as follows: the hTRAIL cDNA clone for

hTRAIL (Trueclone, Cat no. SC126304, OriGene Technologies, Rockville MD) in the vector pCMV6-

XL5, was transfected into mMSCs at passage 3 using OptiMEM® (Gibco) and Lipofectamine LTX Plus

kit (Invitrogen) following manufacturers recommended protocols.  Empty vector transfection was used

to generate mMSC-Vector control cells.  After transfection cells were selected using 300ng/ml G418

(Sigma Aldrich) in media changed every 2 days until colonies were beginning to form.  Cells were then

passaged into 96-well plates, at a confluence of one cell per well, and maintained in selection for 2 wks,

with only one further passage before RNA (qPCR for hTRAIL mRNA levels) and protein (flow

cytometry for surface expression) analysis of constitutive hTRAIL expression and generation of frozen

stocks (50% FBS, 45% Media, 5%DMSO).

Human MSCs were transduced with the TRAIL-IRES-eGFP Lentivirus vector (FLT) as

previously described (22).   The TRAIL-IRES-eGFP lentivirus vector (previously described by

Loebinger  (21, 22) was produced using a lentiviral plasmid (pRRL-cPPT-hPGK-mcs-WPRE) in which

Tet-On system elements had been introduced (generously provided by O. Danos, University College

London), and was then used as a backbone for the incorporation of TRAIL DNA. The existing reporter

gene, MuSEAP, was excised using the MluI and EcoRV restriction sites. The IRES-eGFP sequence

(from pENTR1A) was amplified, and restriction sites were introduced by PCR and then inserted into the

plasmid in place of MuSEAP. Subsequently, human TRAIL (amino acids 1-281; RZPD) was similarly

amplified and restriction sites were introduced by PCR and then cloned into the lentivirus plasmid, via

MluI and BstB1 restriction sites, next to the IRES-eGFP. The plasmid constructs were confirmed by

DNA sequence analysis (Cogenics).

The lentivirus was produced by transfecting 293T cells with 15 mL Opti-Mem, plus 10 mL of a

solution made by mixing 3.6 mL polyethylenimine (Sigma-Aldrich) and 56.4 mL Opti-Mem to 600 Ag

TRAIL plasmid, 450 Ag of the packaging construct pCMV-dR8.74, 150 Ag of a plasmid producing the VSV-G envelope, pMD.G2, and 60 mL Opti-Mem (both pCMV-dR8.74 and pMD.G2 were a kind gift from A. Thrasher, University College London). The lentivirus was concentrated by ultracentrifugation at 18,000 rpm (SW28 rotor, Optima LE80K Ultracentrifuge, Beckman), at 4°C and stored at -80°C before use.  Human MSCs were transduced with a 10-fold multiplicity of infection with 4 Ag/mL polybrene (Sigma-Aldrich), and successful transduction was confirmed by transgene activation.  hTRAIL expression was induced by treatment of cells with 10μg/ml Doxycycline (DOX) (Sigma Aldrich, Stock 10mg/ml).  Cells were treated with DOX every 24 hrs for 3 days, and the surface expression of TRAIL was determined by flow cytometry as described below. TRAIL protein production was further confirmed by ELISA (R&D Systems) according to manufacturer's instructions.  Transduced cells were labeled as hMSC-containing full length TRAIL (hMSC-FLT).  FLT transduced hMSC's, once DOX stimulated, were labeled as hMSC-TRAIL.  FLT transduced hMSCs that were unstimulated were vector controls (hMSC-Vector), and untransduced hMSCs (hMSC-Alone) were used as controls.

## Cell Surface Expression of hTRAIL

Mouse MSC-TRAIL clones 49 and 87, and human MSC-FLT cells +DOX, were trypsinized off the plate and resuspended in 300μl of 1X phosphate buffered saline (PBS).  Samples were fixed for 1 hr in 4% paraformaldehyde (PFA), spun down and resuspended in 1 X PBS, 2% FBS (Flow Buffer (FB)). Cells were washed once in 500μl of FB, with the supernatant poured off at each step. Cells were stained with 1° antibody anti-hTRAIL (ab#2056 Rabbit polyclonal – Abcam, Cambridge, MA) in 200μl of a 1:50 dilution, and incubated at RT for 1hr. Cells were washed 2x in 500μl FB.  Cells were stained with 2° antibody Goat anti Rabbit IgG Alexa 647 (Invitrogen, Life Technologies, Grand Isle, NY) in 200μl of a 1:500 dilution, and incubated, covered, at RT for 30 min. Cells were washed 2x in 500ul FB and

resuspended in 300μl for flow cytometry analysis. An unstained and secondary-only control tube was also stained for each cell line examined.


**Apoptosis detection**

MM cell lines Hmeso and YOU were plated into two six well dished each (50,000 cells per test well 100,000 control well), and allowed to adhere overnight. An extra well was plated on a separate six well dish for compensation controls. MSC cell lines were trypsinized as previously described and counted, and stained in 25uM Cell Tracker Blue –CMAC (Invitrogen, Life Technologies, Grand Isle, NY) for 30 min at 37°C, then cells were spun, and fresh media was placed on the cells, followed by incubation for 30 min at 37°C. Media was changed on the MM cells to remove dead cells caused by plating (2 ml per well). MSCs (25,000 cells) were seeded onto the test wells containing MM cells, and allowed direct coculture for 24 hrs. In an additional well of the compensation controls plate $1 \times 10^5$ Cell Tracker stained hMSCs were seeded. In a 3ml flow cytometry tube, the media was collected for every well, and wells were washed in 500μl of 1X PBS, which was saved and placed in the corresponding tube. Cells were trypsinized with 300μl if Trypsin as previously described, stopped with 1ml of media, and washed thoroughly before collection into the same test tube as the media and wash. All cells were then pelleted by centrifugation in the swinging bucket rotor, at 1200 rpm for 5 minutes at RT.

Cells were stained for early, mid and late apoptosis using the Annexin V PE Apoptosis Detection Kit (eBioscience, San Diego, CA). Cells were washed once in 500μl FB, and once in 500μl 1X Annexin Binding Buffer (ABB) (diluted from 10X stock in the kit with $dH_2O$). Supernatant was poured off and cells were resuspended in the remaining buffer (~ 100μl). Cells were stained with PE conjugated anti-Annexin V (5μl per sample in 100μl 1X ABB), covered, for 15 min at RT. Cells were washed 2x with 500μl of 1X ABB, and resuspended in the residual buffer after pour off. Cells were stained for viability using 7-AAD Viability Staining Solution provided (5μl per sample in 300μl 1X ABB), and cells were

examined by flow cytometry within 4 hours. Single color compensation controls were generated for each stain; MM cells were trypsinized and placed into three tubes, unmodified for unstained, cells fixed for 15 min with 4% PFA for the Annexin V- PE, or fixed 30 min with 4% PFA for 7-AAD Viability stain, and Cell Tracker blue labeled hMSC were trypsinized to a separate tube for the compensation controls. Flow cytometry was performed on a BD LSRII (BD, Franklin Lakes, NJ) following standard protocols, with the exchange of the 610 filter to the 670 filter for reduced overlap of the PE and 7-AAD fluorescence spectra.

Terminal deoxynucleotidyl transferase biotin-dUTP nick end labeling (TUNEL) assay was used to assess tumor cellular apoptosis. Briefly, formalin fixed and paraffin-embedded tissue sections were deparaffinized, hydrated and antigen retrieval was carried out by incubating tissue with Dako target retrieval solution (Dako, Inc, S1699). TUNEL reaction mixture was applied according to manufacturer's instruction (Roche, Inc, 11684817910). For negative controls the transferase enzyme was omitted. The fragmented DNA is stained brown, while DNA without damage is stained blue as a result of counterstaining with hematoxylin.

**Cell differentiation and staining:**

Stem cells were trypsinized as described previously following exposure to MM cell line medias, and MM cell lines, or after expansion of TRAIL expressing clones, and seeded 60,000 per well into a six well dish per cell line/condition, and allowed to adhere overnight. Cells were changed into differentiation media or control media the following day and cultured for three weeks, with media changed two times a week. Osteocyte differentiation media (ODM) and Adipocyte differentiation media (ADM) have been previously described by the Texas A&M Stem Cell Core. Cells were washed in PBS and fixed in 10% formalin for 20 min at RT. Adipose differentiation was washed in PBS the stained with Oil-Red O, Osteogenic differentiation was washed in water, and stained with Alizarin Red, and

stained for 20 min at RT. Wells were washed in the respective buffers until supernatant was clear, and

cells were examined for the presence of adipocytes and osteocytes by microscopy. Images were

captured using an Olympus BX50 upright light microscope (Olympus America, Lake Success, NY) with

an attached Q Imaging Retiga 2000R digital CCD camera (Advanced Imaging Concepts, Inc., Princeton,

NJ).

### *In Vitro* Analysis of Tumorogenicity

MM cell lines and MSC cell lines were trypsinized using 2.5% Trypsin/EDTA (Invitrogen), and counted

using a TC20™ Automated Cell Counter (BioRad, Hurcules, CA). Cells were plated as described below

in their own media, and allowed to adhere overnight before a media change and placing of the transwell

inserts to initiate interaction.

**Proliferation assay:** MM cells were plated in 24 well chambers, 2,000 cells per well. An extra

six well dish was plated with $1 \times 10^6$ cells per well for cell number standard curve. MSCs were plated in

24 well Transwell inserts 0.4 μm pore size, at 1000 cell per insert (Corning Incorporate, Corning, NY).

After 24 hours, plating media was removed by aspiration, experimental media was added (MM cell line

specific), and Transwells containing stem cells were placed in the 24 well dish containing MM cells; this

is day 0. On the experimental day to be analyzed, (4-7), Transwells were removed and media aspirated,

MM cells were trypsinized in 150 μl of trypsin, stopped with 200μl of media. Wells were washed

thoroughly and 100μl was plated in triplicate in a 96 well flat bottom plate. Cells were allowed to settle

to the bottom of the plate for 30 min at 37°C. One well of additional MM cells for the ladder was

trypsinized and counted on BioRad hemacytometer. 200,000 cells in 200μl of media were placed in the

first ladder well, and using serial 1:2 dilutions of 100 μl, a ladder from 100,000 to 1,563 cells in 100μl

was generated, with empty media control wells. Using the CyQuant Proliferation Assay (Invitrogen),

green nucleic acid staining solution was mixed (0.4µl stain, 2.0µl suppressor, in 97.6µl 1x PBS) and 100µl was added to experimental and ladder wells, and incubated at 37°C for 1hr. Live MM cell number was determined using a bottom plate read using a 480/535nm fluorescence reader, with sensitivity set at 60. Fresh ladders were made for every daily plate read using the MM cell line being examined.

**Migration assays:** *Exposure-* MM cell lines were plated 25,000 cells in each well of a six well dish, and allowed to adhere overnight. 15,000 MSC cells were plated in a 6 well transwell chamber insert (0.4µm pore size, Corning Incorporate, Corning, NY), in their own media above and below the membrane and allowed to adhere overnight. Transwell inserts were suspended above the MM cells following a media change in both plates to the MM media at the maximum volume in both chambers, with care taken to aspirate media from the external surface of the transwell, this was day 0. Following 5 days of transwell culture without media change, MM cells were trypsinized as described previously, with an additional wash and change into serum free media, and counted on BioRad hemacytometer. *Effect-* 30,000 MM cells were plated in triplicate into the upper chamber of a 24 well transwell (8.0µm pore size) and placed above MM media containing 20% FBS. Cells were allowed to migrate through the membrane for 24 hrs. Cells remaining on the inside of the Transwell were removed with a sterile cotton swab, and the Transwell was fixed in ice cold methanol for 10 minutes. Transwells were then stained in 0.01% Crytsal Violet in 20% Ethanol for 10 minutes. The Transwell was washed three times in dH$_2$O, and stained cells were lysed in 320µl of 5% methanol, 5% acetic acid in dH$_2$O. Three 100µl aliquots were plated in a flat bottomed 96 well plate and OD$_{595}$ was read by plate reader. One transwell with no cells was used as a negative staining control, to normalize all OD readings.

**Invasion assay:** MM cells were plated as described for the Exposure segment of the migration studies above. On day four of exposure invasion transwells were prepared. Transwell inserts (24 well, 8.0µm pore) were coated with 100µl of BD Matrigel – Basement membrane matrix (cat no.354234 - BD

Biosciences, Franklin Lakes, NJ) in serum free media at a 1:20 dilution, and allowed to air dry overnight. *Effect-* 100,000 MM cells were plated in serum free media into the prepared invasion transwells, and placed above MM media containing 20% FBS. After 24 hours invading cells adherent to the underside of the transwell inserts were fixed and stained as described above, and readings taken at $OD_{595}$.

**Anchorage Independent Growth:** MM cell lines were examined for anchorage independent growth using the Cytoselect™ 96 well Cell Transformation Assay (Cell Biolabs, Inc. San Diego, CA) following the manufacturers protocol with the following modifications. The lower agar layer was prepared as written, plated and allowed to set at 4°C for 30 min. Cell lines were trypsinized and counted as described previously, then resuspended at $1 \times 10^6$ cells per ml. Cell mixtures were aliquoted into test tubes at a maximum volume of 25µl in media (enough for 5 wells), and incubated at 37°C for 30 minutes. The cell agar layer was prepared as described without the cell addition, then 350µl was aliquoted into the cell mixture tubes. Cell agar layers were incubated for 10 min at 37°C. The warm cell agar layer was plated in triplicate (75µl) onto the base agar layer and incubated at 4°C, methods then proceeded as written in the protocol. Control wells of MM cells alone were plated at an equal number of cells as the number of MM cells within the cell mixtures, MSC cells alone were plated the same.

**SCID Mouse Xenograft Model of Human Malignant Mesothelioma**

All animal procedures were approved by the UVM IACUC and conformed to all appropriate institutional and AAALAC standards. A previously established model of intraperitoneal inoculation of human Hmeso cells into SCID mice was utilized (2). In brief, for both the MSC localization to tumor and early tumor development models, $5 \times 10^6$ Hmeso cells (in 150µl sterile 0.9% NaCl [pH 7.4]) were injected IP into male, 6 week old Fox Chase SCID mice from Charles River Laboratories (Strain number 236). Injections were administered to the lower left anterior of the mice (1 injection site/mouse). An

extra aliquot of Hmeso cells was replated in a 25 cm$^2$ culture flask after injections to verify cell viability. Ear punches were administered as needed to distinguish between animals. All animal procedures were approved by the IACUC committee at UVM. Both free-floating spheroid and mesenchymal tumors lining the diaphragm were observed at 28 days in all mice at which time saline (n=5), or 1 x 10$^6$ MSC cells in 500 μl sterile 0.9% NaCl (pH 7.4) were injected either systemically (intraveinous – tail vein [IV] (n=5)) and locally (intraperitoneal [IP] (n=5)), for 24 hr for the localization analysis (Figure 2), or MSCs as described were administered IP on Day 7 and Day 14 of tumor development (n=8; saline n=7), with tumor burden measured on day 28, for the early tumor development model (Figure 3).

MSCs as a cell based therapy experiments used a modification of the above model, to allow a greater therapeutic window. In brief, 1 x 10$^6$ Hmeso cells (in 150 μl sterile 0.9% NaCl [pH 7.4]) were injected into SCID mice as described above. Mesenchymal tumors throughout the IP cavity were observed by 28 days in all mice. Mice were treated by IP injection with either 1x PBS, or 3 x 10$^5$ MSC cells in 300μl sterile 1x PBS, beginning on day 21, and receiving two injections per week for three weeks (Figure 5 and Supplemental Figure 2). Mice received either control injections of saline (n=6), MSC-Alone (unmodified mMSC or hMSCs (n=8 each)); MSC-Vector cells (mMSCs transfected with empty vector pCMV6-XL5 (n=8), or hMSC-FLT cells not stimulated with DOX (n=8)); or MSC-TRAIL cells (mMSC-TRAIL clone 87 (n=8), or hMSC FLT cells stimulated for 72hr with DOX (n=8)). Tumor burden assessment was performed on day 46 of tumor growth. To correct for any cell growth differences, hMSC-FLT cells were grown for simultaneous Vector and TRAIL injection, and in each plating, half of the cells would receive DOX treatment. MSC origin is indicated by a preceding lower case m (mouse) or h (human). Tumor burden assessment was performed on day 46, and was determined by collection of all tumors, including any small metastatic nodes, with detailed examination of pleural cavity, diaphragm, liver, stomach, spleen, intestines, kidney, reproductive organs, and subcutaneous area proximal to MM injection site for metastasis, with weight and volume recorded for all tumors. No

difference was observed when comparing weight and volume data, thus weight is depicted. Tumors were defined as either spheroid: free floating within the peritoneal cavity; or mesenteric: attached to the mesentery. Day 46 spheroid tumors were never observed.

**Assessment of peritoneal inflammation**

Mice were euthanized with 0.1ml of Sleep Away (26% sodium pentobarbital, Webster Veterinary), and peritoneal lavage fluid (PLF) was collected as previously described (2, 32). 3ml of cold 1X PBS was instilled into the peritoneal cavity of each mouse using an 18g needle. The abdomen was then lightly massaged, and the PBS removed. Recovered volume was recorded, and samples were centrifuged to pellet cells. The supernatants were collected and soluble inflammatory cytokine levels were assayed in PLF and cell culture media supernatants using Bio-plex Pro™ Mouse Cytokine 23-plex Assay and Bio-plex Pro™ Human Cytokine 27-plex Assay (BioRad), using manufacturers recommended protocol. Cell pellets were treated with 3ml ACK Lysis buffer (Gibco) for 30 sec to remove red blood cells, and lysis was halted by addition of 8ml 1X PBS. Cells were pelleted and re-suspended in 600µl 1X PBS and the total white blood cell counts in PLF were assessed using an ADVIA® Hematology Analyzer (Siemens Diagnostics, Johnson City, TN). Cytospins were prepared from $5 \times 10^5$ cells following standard protocols (30). Cytospins were stained using a HEMA 3 kit (Fisher Scientific, Middletown, VA) per the manufacturer's directions.

**Immunofluorescence microscopy detection of GFP-MSCs**

Immunofluoresence visualization of the GFP-Alexa-555 antibody was performed on sections of paraffin-embedded Mesenteric Hmeso tumors derived from 2 IV-injected mice, 2 IP-injected mice and 2

Saline control mice. Sections were deparaffinized in xylenes followed by hydration in $dH_2O$ via decreasing alcohol concentrations. Antigen retrieval was performed by placing slides in 1X Dako target retrieval solution at 98-99°C for 20min (Dako, Carpinteria, CA). Slides were then cooled to room temperature before auto-fluoresence was blocked with 10% bovine serum albumin BSA (Sigma) in 1X PBS for 10min. Sections were incubated for 15 min in 0.1% Triton-X (Sigma) in 1% BSA, 1X PBS solution, followed by two 5min washed in 1X PBS. Mouse anti-GFP-Alexa-555 antibody (Invitrogen) was diluted 1:200 in 1% BSA (Sigma) in 1X PBS. Tumor sections were treated with diluted primary antibody overnight in a humidified chamber at 4°C. A 1:10,000 dilution of DAPI nucleic acid stain (Molecular Probes, Life Technologies, Grand Isle, NY) in 1X PBS was then applied to each section for 5min. Slides were washed with 1X PBS before adherence of coverslips (Aqua Poly/Mount, Polysciences Inc., Warrington, PA), and stored at 4°C. Confocal images of 2-3 fields per tumor or intestine were acquired using a 40X objective lens on a BioRad MRC 1024ES confocal scanning laser microscope running BioRad Lasersharp 2000 imaging software (Advanced Imaging Concepts, Inc.). A triple fluorescence mode was used to visualize cell nuclei (blue) and GFP fluorescence (green – not shown in confocal images) and Anti-GFP Alexa-555 (red) in tissues. Images were scanned in sequential mode to avoid bleed- through between channels. Images were acquired sequentially then were pseudo colored and merged.

**RNA isolation, cDNA conversion, qPCR**

RNA was isolated from A549, mMSC, and mMSC-TRAIL cells by Trizol (Invitrogen), converted to cDNA using BioRad iScript cDNA synthesis kit (BioRad, Hercules, CA), and quantified using IQ SyberGreen (BioRad), per manufacturers recommended protocol. Cells were trypsinized as described above and pelleted, supernatant was removed, and pellet resuspended in a small volume. 500µl of Trizol (Invitrogen, Life Technologies, Grand Island, NY) was added and mixed. 100µl of 1-

bromo-3-chloropropane (BCP) (Molecular Research Center, Cincinnati, OH) was added to each tube, and the sample was vortexed. Tubes were spun for 5 minutes at 12 thousand RPM in a fixed angel rotor. Aqueous phase was isolated into a new tube without dislodging protein fraction layer. Saturated ammonium chloride (25µl) was added to the tube to facilitate RNA precipitation, and 500µl of isopropanol, Samples were mixed and incubated for 20 min at -20°C. Samples were spun to pellet RNA, supernatant aspirated, and washed 1x in 70% ethanol. RNA pellet was air dried for 5-10 minutes but not completely dried, and sample was resuspended in 40µl of Rnase Free $dH_2O$. Concentration was dertermined by Nanodrop.

RNA was converted to cDNA using BioRad iScript cDNA synthesis kit (BioRad, Hercules, CA) following manufacturers recommended protocol, using 800ng of RNA per 20µl reaction. IQ SyberGreen (BioRad, Hercules, CA) qPCR amplification of human TRAIL mRNA was performed in 25µl reactions following recommended protocols on 10µg of converted cDNA (calculated) using the following primers hTRAIL- F 5'-TTTCGGGGCCTTTTTAGTTGG-3', R 5'-ACTTGAGAGATGGATTGTTGC-3', and GapdH F 5'-ACGACCCCTTCATTGACCTC -3', R 5'-TTCACACCCATCACAAACAT -3'. Control RNA was isolated from an abundance of A549 cells, aliquots were used as a cDNA conversion efficiency control and on converted sample 2µg in 40µl was used subsequently to generate a cDNA ladder which was run for primer efficiency on every plate. Comparisons between plates were normalized to the ladder. PCR was run with standard conditions and an annealing temperature set at 56°C, with 10s, 15s, and 20s times for denaturing, annealing, and extension respectively. Melt curve from 40-95°C was used to examine amplicon purity.

**Statistical analysis**

All data were evaluated by analysis of variance (ANOVA) using the Fishers LSD procedure for adjustment of multiple comparisons to the Saline treatment groups. Where appropriate Students T-test

using Welch's correction was used (33). Statistical significance was determined as $p \leq 0.05$= single, $p \leq 0.01$= double, $p \leq 0.001$= triple symbols. Significance of any treatments compared to Saline controls is indicated by *, significance between MSC-TRAIL cells and other MSC cell controls is indicated by # and @ at the $p \leq 0.05$ level. Any p-values approaching significance noted in the figures are in reference to comparisons with Saline controls only.